Electronic Supplementary Material (ESI) for ChemComm.

Supporting Information

Dynamic covalent assembly and disassembly of nanoparticle aggregates

Stefan Borsley and Euan R. Kay

1. General experimental procedures 2
2. Synthesis of organic compounds 3
3. Nanoparticle synthesis and characterization 7
3.1 AuNP-1 7
3.2 AuNP-S3 10
4. NP-bound boronate ester formation and equilibration 12
4.1 Relaxation time measurements 12
4.2 Boronate ester response to base concentration 13
4.3 Titrations to establish NP-bound boronate ester surface saturation 14
4.3.1 Nanoparticle-bound boronate ester modelling 15
4.4 Approaching equilibrium via different pathways 18
4.4.1 NP-Bound boronate ester equilibration at high Lewis base concentration 18
4.4.2 NP-Bound boronate ester equilibration at low Lewis base concentration 21
4.5 Cyclable boronate ester equilibration 22
5. Nanoparticle assembly 23
5.1 Assembly with linker 6 or 7 23
6.2 Control NP assembly experiments 27
5.2.1 Stability of AuNP-1 27
5.2.2 Control AuNP-S3 28
5.3 NP Aggregate disassembly 29
7. ^{1}H and ^{13}C NMR spectra of organic compounds 31
9. References 37

1. General experimental procedures

Unless stated otherwise, all reagents were purchased from commercial sources (Sigma Aldrich UK, Alfa Aesar UK, Acros UK or Apollo Scientific) and used without further purification. Dry solvents were obtained by means of a MBBRAUN MB SPS-800^{TM} solvent purification system, where solvents were passed through filter columns and dispensed under an argon atmosphere. Flash column chromatography was performed using Geduran® Si60 (40-63 µm, Merck, Germany) as the stationary phase, and thin-layer chromatography (TLC) was performed on pre-coated silica gel plates (0.25 mm thick, 60F_{254}, Merck, Germany) and observed under UV light (λ_{max} 254 nm), or visualized by staining with a basic potassium permanganate solution, followed by heating. AuNP micrographs were obtained using a JEM 2010 transmission electron microscope (TEM) on samples prepared by deposition of one drop of nanoparticle suspension on Holey Carbon Films on 300 mesh Cu grids (Agar Scientific®). NP diameters were measured automatically using the software *ImageJ*. The images were first converted to black and white images using the "Threshold" function. The area of the NPs was measured using the "Analyze particles" function. Particles on edges were excluded. UV-vis spectroscopy was performed using a Thermo Scientific Evolution 220 UV-Visible Spectrophotometer. ^{1}H, ^{13}C, and ^{31}P NMR spectra were recorded on Bruker Avance II 300, 400 and 500 instruments, at a constant temperature of 25 °C. ^{1}H chemical shifts are reported in parts per million (ppm) from low to high field and referenced to the literature values for chemical shifts of residual non-deuterated solvent, with respect to tetramethylsilane. ^{19}F chemical shifts are referenced to CF_3Cl (0.00 ppm) as external standard. ^{31}P NMR chemical shifts are referenced to PPh_3 (–6.00 ppm) as external standard. Standard abbreviations indicating multiplicity are used as follows: bs (broad singlet), d (doublet), dd (doublet of doublets), m (multiplet), q (quartet), s (singlet), t (triplet), tt (triplet of triplets), *J* (coupling constant). All spectra were analyzed using MestReNova (Version 9.0.0). All melting points were determined using a Stuart SMP30 Melting Point Apparatus and are reported uncorrected. Multielement inductively coupled plasma optical emission spectroscopy (ICP-OES) was performed using a Perkin Elmer Optima 5300 DV, employing an RF forward power of 1400 W, with argon gas flows of 15, 0.2 and 0.75 L min^{-1} for plasma, auxiliary, and nebuliser flows, respectively. Using a peristaltic pump, sample solutions were taken up into a Gem Tip cross-flow nebuliser and the instrument was operated in axial mode for all elements. A range of calibration standards were prepared using single element 1000 mg L^{-1} stock solutions for Au, B and S (Fisher Scientific UK LTD), diluted with 3% *v*/*v* aqua regia. The selected wavelengths for each element were analysed in fully quant mode (three points per unit wavelength). Three replicate runs per sample were employed.

2. Synthesis of organic compounds

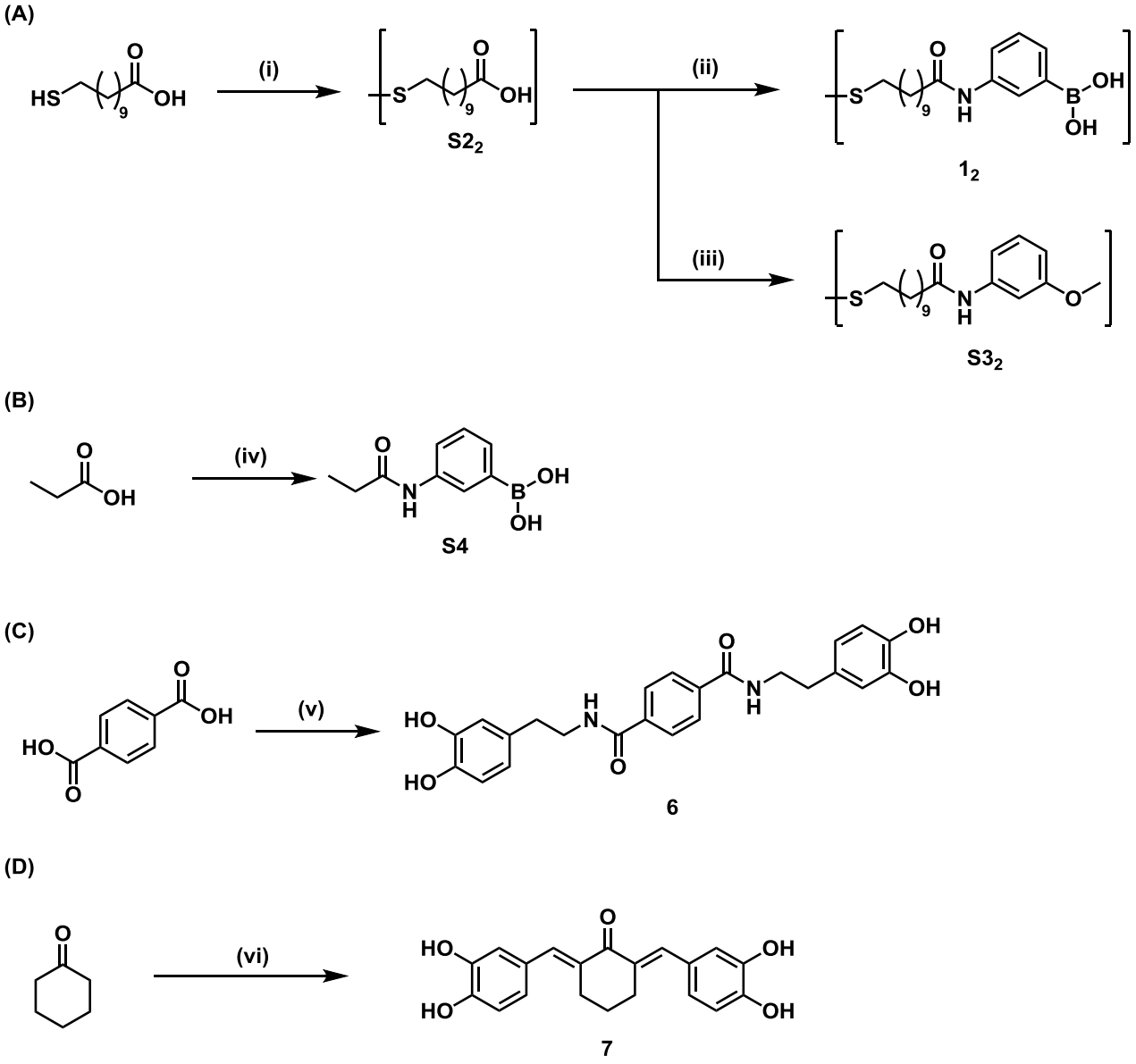

Scheme S1 Reagents and conditions for synthesis of compounds **1_2**, **$S3_2$**, **S4**, **6** and **7.** (i) SO_2Cl_2, CH_2Cl_2, 0 °C, 0.1 h, 99%. (ii) 3-Aminophenylboronic acid monohydrate, 1-ethyl-3-(3-dimethylaminopropyl)carbodiimide hydrochloride (EDC•HCl), HOBt, *N*,*N*-diisopropylethylamine, MeCN/THF, r.t., 18 h, 82%. (iii) 3-Methoxyaniline, EDC•HCl, HOBt, *N*,*N*-diisopropylethylamine, MeCN/THF, r.t., 18 h, 77%. (iv) 3-Aminophenylboronic acid monohydrate, EDC•HCl, H_2O, r.t., 24 h, 47%. (v) Dopamine hydrochloride, EDC•HCl, HOBt, *N*,*N*-diisopropylethylamine, DMF, r.t., 16 h, 94%. (vi) 3,4-Dihydroxybenzaldehyde, HCl/H_2O, AcOH, 50 °C, 3 h, 31%.

Compound S1: Chloro(triphenylphosphine)gold(I)

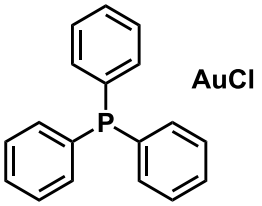

A solution of PPh_3 (735 mg, 2.80 mmol) in diethyl ether (10 mL) was added dropwise to a solution of $HAuCl_4 \cdot 3H_2O$ (500 mg, 1.47 mmol) in diethyl ether (30 mL). The reaction mixture was stirred at 0 °C for three hours, and then allowed to warm to room temperature. The resulting white precipitate was filtered and washed with cold Et_2O to give an off-white solid. This solid was recrystallized from CH_2Cl_2/hexane to give the desired gold complex **S1** as a crystalline white solid (500 mg, 1.01 mmol, 69%). m.p.: 236–237 °C; ^{1}H NMR (300.1 MHz, $CDCl_3$): δ 7.55–7.45 (15H, m, Ar*H*); ^{13}C NMR (125.8 MHz, $CDCl_3$): δ = 134.3 (d, *J* = 13.7 Hz), 132.2 (d, *J* = 2.5 Hz), 129.4 (d, *J* = 11.8 Hz), 129.3 (d, *J* = 96.7 Hz); ^{31}P NMR (121.5 MHz, $CDCl_3$): δ = 33.5 (1P, s); HRMS (ES^+) *m/z* calculated for $[M+Na]^+$ $C_{18}H_{15}AuClNaP$ 517.0158, found 517.0162.

Compound $S2_2$: 11,11'-disulfanediyldiundecanoic acid

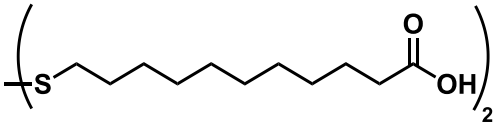

A solution of sulfuryl chloride (1.24 g, 0.77 mL, 9.16 mmol) in dry CH_2Cl_2 (30 mL) was added to a solution of 11-mercaptoundecanoic acid (4.00 g, 18.3 mmol) in dry CH_2Cl_2 (60 mL) at 0 °C. Solvent was removed under vacuum to give the desired product **$S2_2$** as an off-white solid (3.99 g, 9.18 mmol, 99%, spectral data in agreement with the literature[S1]). m.p.: 97–100 °C; ^{1}H NMR (300.1 MHz; DMSO-d_6): δ = 2.68 (4H, t, *J* = 6.0, CH_2S), 2.18 (4H, t, *J* = 7.5, 2 × CH_2CO$_2$H) 1.65–1.55 (4H, m, 2 × CH$_2$CH_2S), 1.52–1.43 (4H, m, CH_2), 1.38– 1.20 (24H, m, 12 × CH_2); ^{13}C NMR (75.5 MHz; DMSO-d_6): δ = 174.5 (*C*), 37.8 (*C*H$_2$), 33.6 (*C*H$_2$), 28.8 (*C*H$_2$), 28.8 (*C*H$_2$), 28.8 (*C*H$_2$), 28.7 (*C*H$_2$), 28.5 (*C*H$_2$), 28.5 (*C*H$_2$), 27.7 (*C*H$_2$), 24.5 (*C*H$_2$).

Compound 1_2: (((11,11'-disulfanediylbis(undecanoyl))bis(azanediyl))bis(3,1- phenylene))diboronic acid

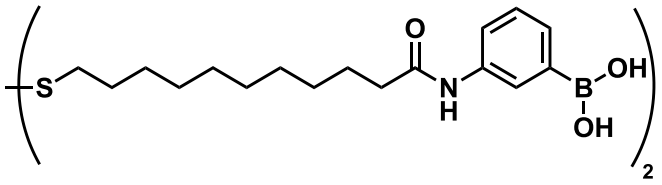

11,11'-Disulfanediyldiundecanoic acid (**$S2_2$**) (1.00 g, 2.30 mmol), 3-aminophenylboronic acid monohydrate (0.891 g, 5.75 mmol) and EDC·HCl (1.10 g, 5.75 mmol) were dissolved in THF (10 mL) and MeCN (10 mL). *N*,*N*-Diisopropylethylamine (1.49 g, 11.5 mmol) was added and the reaction was stirred at room temperature for 16 hours. The solution was poured into a mixture of EtOAc and 1 M HCl, and allowed to stand for 2 hours, during which time a white solid precipitated at the phase boundary. The solid was filtered, washed with 1M HCl and CH_2Cl_2 and dried under vacuum to afford the desired product **1_2** as an off white solid (1.26 g, 1.88 mmol, 82%). m.p.: 204–209 °C (dec.); ^{1}H NMR (500.1 MHz; DMSO-d_6): δ = 9.78 (2H, s, N*H*), 7.81 (2H, s, Ar*H*), 7.71 (2H, d, *J* = 8.2, Ar*H*), 7.45 (2H, d, J = 7.2, 2 × Ar*H*), 7.23 (2H, t, *J* = 9.0, Ar*H*), *2*.67 (4H, t, *J* = 7.2, *CH*$_2$S), 2.27 (4H, t, *J* = 7.4, *CH*$_2$CO) 1.64–1.51 (8H, m, C*H*$_2$), 1.38–1.19 (24H, m, C*H*$_2$); ^{13}C NMR (125.8 MHz; DMSO-d_6): δ = 171.3 (*C*), 138.6 (*C*), 132.5 (*C*), 128.9 (*C*H), 127.8 (*C*H), 125.2 (*C*H), 121.2 (*C*H), 37.9 (*C*H$_2$), 36.5 (*C*H$_2$), 29.0 (*C*H$_2$), 29.0 (*C*H$_2$), 28.9 (*C*H$_2$), 28.8 (*C*H$_2$), 28.7 (*C*H$_2$), 28.6 (*C*H$_2$), 27.8 (*C*H$_2$), 25.3 (*C*H$_2$); HRMS (ES$^+$) *m/z* calculated for dimethoxy ester derivative $[M+2CH_2+H]^+$ $C_{36}H_{58}B_2N_2O_6S_2^+$ 723.3815, found 723.3802.

Compound $S3_2$: 11,11'-disulfanediylbis(N-(3-methoxyphenyl)undecanamide)

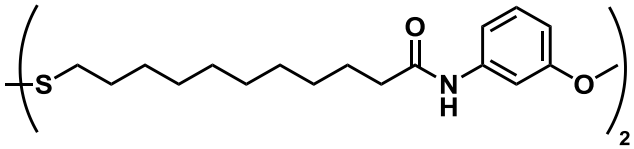

11,11'-Disulfanediyldiundecanoic acid (**$S2_2$**) (1.00 g, 2.30 mmol), 3-methoxyaniline (0.708 g, 5.75 mmol) and EDC·HCl (1.10 g, 5.75 mmol) were dissolved in THF (10 mL) and MeCN (10 mL). *N*,*N*-diisopropylethylamine (1.49 g, 11.5 mmol) was added and the reaction was stirred at room temperature for 16 hours. The solution was poured into a mixture of EtOAc and 1 M HCl. A white solid precipitated instantaneously at the phase-boundary. The solid was filtered, washed with 1M HCl and CH_2Cl_2 and dried under vacuum to afford the desired product **$S3_2$** as a white solid (1.14 g, 1.77 mmol, 77%). ^{1}H NMR (500.1 MHz; DMSO-d_6): δ = 9.83 (s, 2H, N*H*), 7.30 (t, *J* = 2.2 Hz, 2H, Ar*H*), 7.17 (t, *J* = 8.1 Hz, 2H, Ar*H*), 7.10 (dt, *J* = 8.3, 1.2 Hz, 2H, Ar*H*), 6.59 (ddd, *J* = 8.1, 2.5, 1.0 Hz, 2H, Ar*H*), 3.71 (s, 6H, C*H*$_3$), 2.67 (t, *J* = 7.2 Hz, 4H, C*H*$_2$), 2.27 (t, *J* = 7.4 Hz, 4H, C*H*$_2$), 1.58 (dq, *J* = 16.0, 8.3, 7.7 Hz, 8H, C*H*$_2$), 1.32–1.22 (m, 24H,C*H*$_2$); ^{13}C NMR (125.8 MHz; DMSO-d_6): δ = 171.3 (*C*), 159.5 (*C*), 140.6 (*C*), 129.4 (*C*H), 111.3 (*C*H), 108.3 (*C*H), 104.8 (*C*H), 54.9 (*C*H$_3$), 37.9 (*C*H$_2$), 36.5 (*C*H$_2$), 28.9 (*C*H$_2$), 28.9 (*C*H$_2$), 28.8 (*C*H$_2$), 28.7 (*C*H$_2$), 28.6 (*C*H$_2$), 28.5 (*C*H$_2$), 27.5 (*C*H$_2$), 25.1 (*C*H$_2$); HRMS (ES$^+$) *m/z* calculated for $[M+Na]^+$ $C_{36}H_{56}N_2O_4S_2Na^+$ 667.3574, found 767.3576.

Compound S4: (3-propionamidophenyl)boronic acid

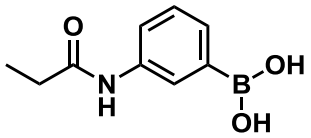

3-Aminophenylboronic acid monohydrate (0.500 g, 3.65 mmol) was dissolved in water (30 mL) and EDCI·HCl (1.05 g, 5.48) was added. To this solution, propanoic acid (2.76 mL, 36.5 mmol) was added. The mixture was stirred at room temperature for 24 h then extracted with Et_2O (3 × 35 mL). Solvent was removed under reduced pressure and the residue was recrystallised from water to yield the desired product **S4** as a white crystalline solid (0.360 g, 1.87 mmol, 47%). ^{1}H NMR (500.1 MHz, DMSO-d_6): δ = 9.77 (1H, s, N*H*), 7.99 (2H, s, O*H*), 7.81 (1H, s, Ar*H*), 7.71 (1H, d, *J* = 9.0 Hz, Ar*H*), 7.44 (1H, d, *J* = 7.5 Hz, Ar*H*), 7.24 (1H, 8.0 Hz, Ar*H*)**,** 2.30 (2H, q, *J* = 7.5 Hz, CH_2), 1.07 (3H, t, *J* = 7.5 Hz, CH_3); ^{13}C NMR (75.5 MHz, DMSO-d_6): δ = 171.8 (*C*), 138.51 (*C*), 132.6 (*C*), 128.7 (*C*H), 127.6 (*C*H), 125.1 (*C*H), 121.1 (*C*H), 29.5 (CH_2), 9.8 (CH_3). HRMS (ES$^+$) *m/z* calculated for monomethoxy-derivative $[M+CH_2+H]^+$ $C_{10}H_{15}BNO_3^+$ 208.1140, found 208.1147.

Compound 6: *N*^{1},*N*^{4}-bis(3,4-dihydroxyphenethyl)terephthalamide

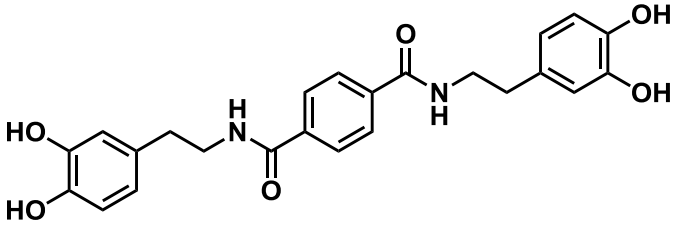

Terephthalic acid (500 mg, 3.01 mmol), dopamine hydrochloride (1490 mg, 7.52 mmol), EDC.HCl (1442 mg, 7.52 mmol) and HOBt (1016 mg, 7.52 mmol) were dissolved in DMF (20 mL) under argon. *N*,*N*-Diisopropylethylamine (2917 mg, 22.6 mmol) was added and the reaction was stirred at room temperature for 16 hours. The reaction mixture was poured into 1 M HCl (100 mL) and left to stand for 1 hour. After 1 hour a while solid had precipitated. The solid was filtered, washed with 1M HCl and dried under vacuum to give the desired product **6** as a white solid (1.24 g, 2.83 mmol, 94%); M.p.: 230–232 °C; ^{1}H NMR (300.1 MHz; DMSO-d_6): δ = 8.64 (t, *J* = 5.6 Hz, 2H), 7.88 (s, 4H), 6.68–6.58 (m, 4H), 6.47 (dd, *J* = 8.0, 2.1 Hz, 4H), 3.39 (dt, *J* = 8.6, 6.2 Hz, 4H), 2.65 (dd, *J* = 8.7, 6.4 Hz, 4H); ^{13}C NMR (75.5 MHz; DMSO-d_6): δ = 164.4 (2*C*), 145.1 (2*C*), 143.6 (2*C*), 136.8 (2*C*), 130.2 (2*C*), 127.1 (4*C*H), 119.3 (2*C*H), 116.0 (2*C*H), 115.5 (2*C*H), 41.4 (2*C*), 34.6 (2*C*); HRMS (NSI$^+$) m/z calculated for $C_{24}H_{25}N_2O_6$ $[M+H]^+$ 437.1707, observed 437.1706.

Compound 7: 2,6-bis((E)-3,4-dihydroxybenzylidene)cyclohexan-1-one

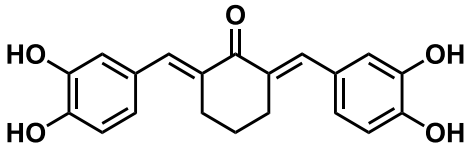

3,4-Dihydroxybenzaldehyde (464 mg, 3.36 mmol) and cyclohexanone (150 mg, 1.53 mmol) were dissolved in acetic acid (20 mL). Concentrated HCl (2 mL) was added and the mixture was stirred at 50 °C for 3 hours. The solution turned dark red. Water (100 mL) was added, precipitating a black solid, which was recovered by filtration. The product was recrystallised from MeOH/H_2O to give the desired product **7** a fine golden crystalline solid (158 mg, 0.467 mmol, 31%); M.p.: 242–246 °C (dec.); ^{1}H NMR (300.1 MHz; DMSO-d_6): δ = 9.45 (s, 2H, O*H*), 9.15 (s, 2H, O*H*), 7.45 (s, 2H, *CH*), 6.98 (d, *J* = 2.0 Hz, 2H, Ar*H*), 6.93–6.75 (m, 4H, Ar*H*), 2.85 (t, *J* = 5.8 Hz, 4H, CH_2), 1.71 (m, 2H, CH_2); ^{13}C NMR (75.5 MHz; $CDCl_3$): δ = 188.5 (*C*), 146.8 (2*C*), 145.1 (2*C*), 136.1 (2*C*H), 133.1 (2*C*), 126.9 (2*C*), 123.4 (2*C*H), 117.6 (2*C*H), 115.7 (2*C*H), 28.1 (2*C*H_2), 22.5 (*C*H_2); HRMS (ES^-) m/z calculated for $C_{20}H_{17}O_5$ $[M-H]^-$ 337.1081, observed 337.1080.

3. Nanoparticle synthesis and characterization

3.1 AuNP-1

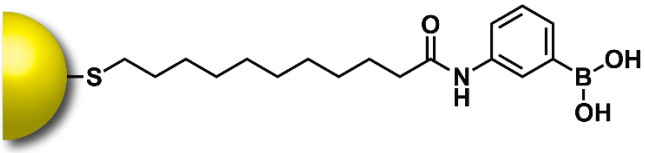

Synthetic procedure

$ClAuPPh_3$ (**S1**) (1000 mg, 2.02 mmol), boronic acid-disulfide $\mathbf{1_2}$ (820 mg, 1.21 mmol) and butylated hydroxytoluene (668 mg, 3.03 mmol) were dissolved in a mixture of THF/MeOH (10:1 *v*/*v*, 220 mL) and stirred at 55 °C. To this, borane *tert*-butylamine complex (1760 mg, 20.2 mmol) was added as a powder. The mixture was stirred for 1 hour at 55 °C. After this time, the solution was allowed to cool to RT and stirred for a further 5 hours. Et_2O (≈ 400 mL) was added and the reaction mixture was then concentrated *in vacuo* until a black precipitate formed. The clear supernatant was discarded and the solid was washed consecutively with 0.1 M HCl, THF, CH_2Cl_2 and Et_2O. The solid was re-suspended in THF/MeOH (10:1 *v*/*v*, 50 mL) to give a black/red colloidal solution, and precipitated by addition of Et_2O and washed again with the same solvents. The precipitation/washing cycle was repeated with the same steps a total of 5 times, after which the black solid was dried *in vacuo* to give the desired nanoparticles AuNP-**1** as a black powder (382 mg).

Characterization

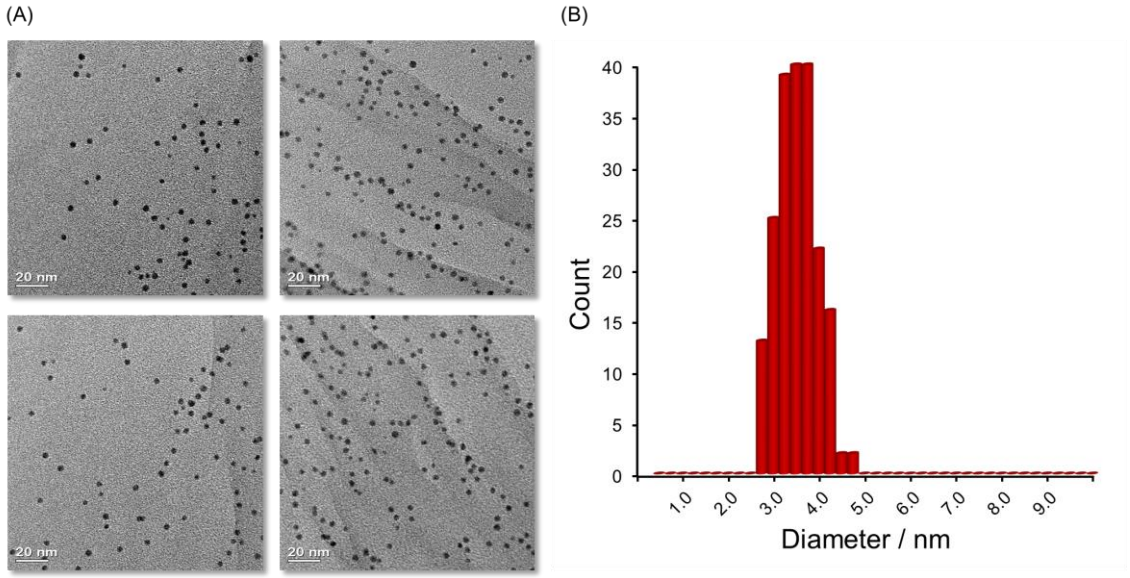

Figure S1 (**A**) Representative TEM images of AuNP-**1** and (**B**) histogram of NP size distribution as found through analysis of several images using ImageJ software, as described in the general methods section. AuNP-**1** were found to have a size of 3.41 ± 0.43 nm, corresponding to a dispersity of 13%.

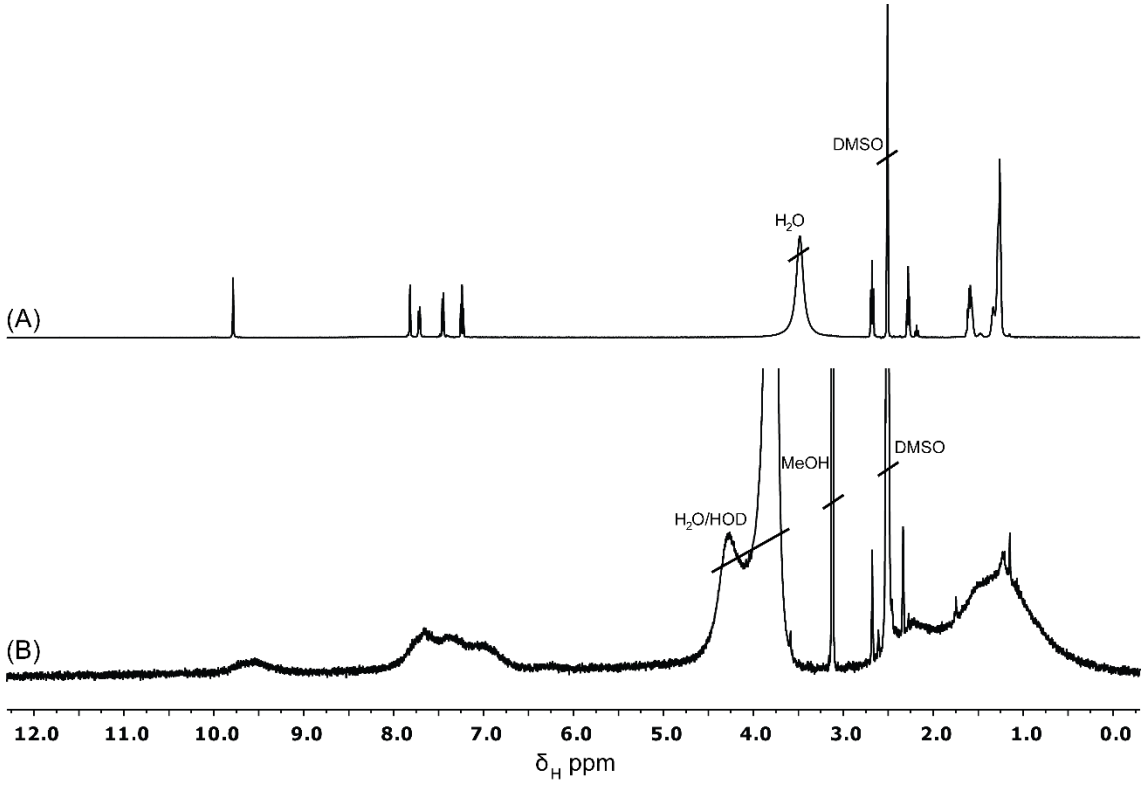

Figure S2 ^{1}H NMR spectra of (**A**) boronic acid disulfide ligand $\mathbf{1_2}$ (DMSO-d_6, 400.1 MHz, 298 K) and (**B**) boronic acid-coated AuNP-**1** (DMSO-d_6/H_2O, 99:1 *v*/*v*, 400.1 MHz, 298 K).

Oxidative ligand strip of AuNP-1: AuNP-**1** and 3-fluoro-4-bromonitrobenzene were dissolved in DMSO-d_6/D_2O, 99:1 (1 mL) and a few pellets of iodine were added. The solution was subsequently analysed by ^{1}H NMR spectroscopy (**Figure S3**).

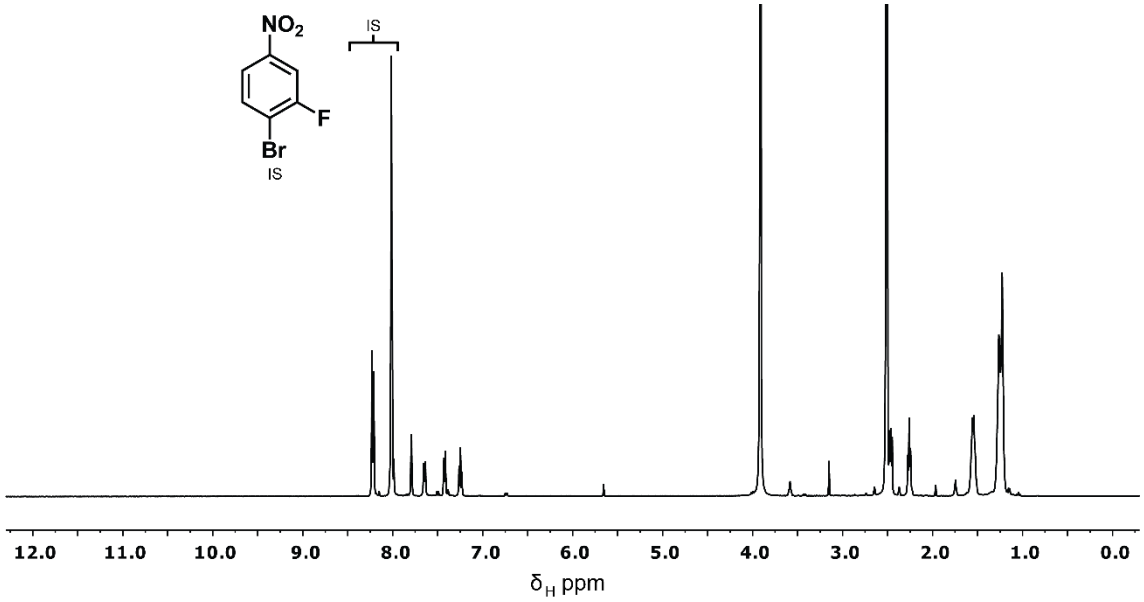

Figure S3 ^{1}H NMR spectrum (DMSO-d_6/D_2O, 99:1 *v*/*v*, 500.1 MHz, 298 K) of AuNP-**1** and internal standard (3-fluoro-4-bromonitrobenzene **IS**), ca. 5 minutes after addition of iodine.

ICP-OES analysis of AuNP-1: AuNP-**1** was dissolved in conc. HCl / conc. HNO_3 (3:1 *v*/*v*, 1.2 mL, freshly prepared from analytical grade reagents). Once the nanoparticles had fully dissolved, the sample was diluted with water (10 mL) to give a total volume of 11.2 mL. Blank samples were prepared in the same way, but without the addition of NPs. Absolute gold, sulfur and boron concentrations were determined in ppm by subtracting the blank from the measured sample. The results summarised in **Table S1** are for two independently prepared repeats; three replicate runs were performed on each.

Table S1 ICP-OES data for AuNP-**1**.

	Repeat A	**Repeat B**
Mass AuNP-1 /mg	1.99	2.60
Sample volume /mL	11.2	11.2
Au /ppm	120.31	156.16
S /ppm	2.74	3.45
B /ppm	0.89	1.13
Mass Au /mg	1.35	1.75
Mass S /mg	0.031	0.039
Mass B /mg	0.010	0.013
Au content /μmol	6.84	8.88
S content /μmol	0.956	1.20
B content /μmol	0.921	1.17
Au:S:B molar ratio	7.2 : 1.0 : 0.96	7.4 : 1.0 : 0.97

3.2 AuNP-S3

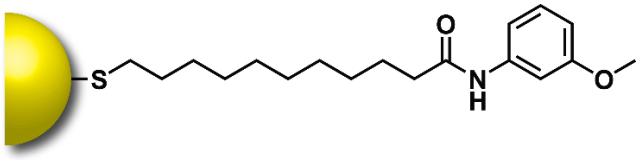

Synthetic procedure

$ClAuPPh_3$ (**S1**) (50 mg, 0.101 mmol) and methyl ether-disulfide **$S3_2$** (39 mg, 0.0605 mmol) were dissolved in a mixture of THF/MeOH (10:1 *v*/*v*, 11 mL) and stirred at 55 °C. To this, borane *tert*-butylamine complex (88 mg, 1.01 mmol) was added as a powder. The mixture was stirred for 1 hour at 55 °C. After this time, the solution was allowed to cool to RT and stirred for a further 5 hours. Et_2O (≈ 400 mL) was added and the reaction mixture was then concentrated *in vacuo* until a black precipitate formed. The

clear supernatant was discarded and the solid was washed consecutively with 0.1 M HCl, and CH_2Cl_2. The solid was suspended in THF/MeOH (10:1 *v*/*v*, 10 mL) to give a black/red colloidal solution, and precipitated by addition of ether/concentration *in vacuo*, and washed again with the same solvents. The precipitation/washing cycle was repeated with the same steps a total of 5 times, after which the black solid was dried *in vacuo* to give the desired nanoparticles AuNP-**S3** as a black powder (21 mg).

Characterization

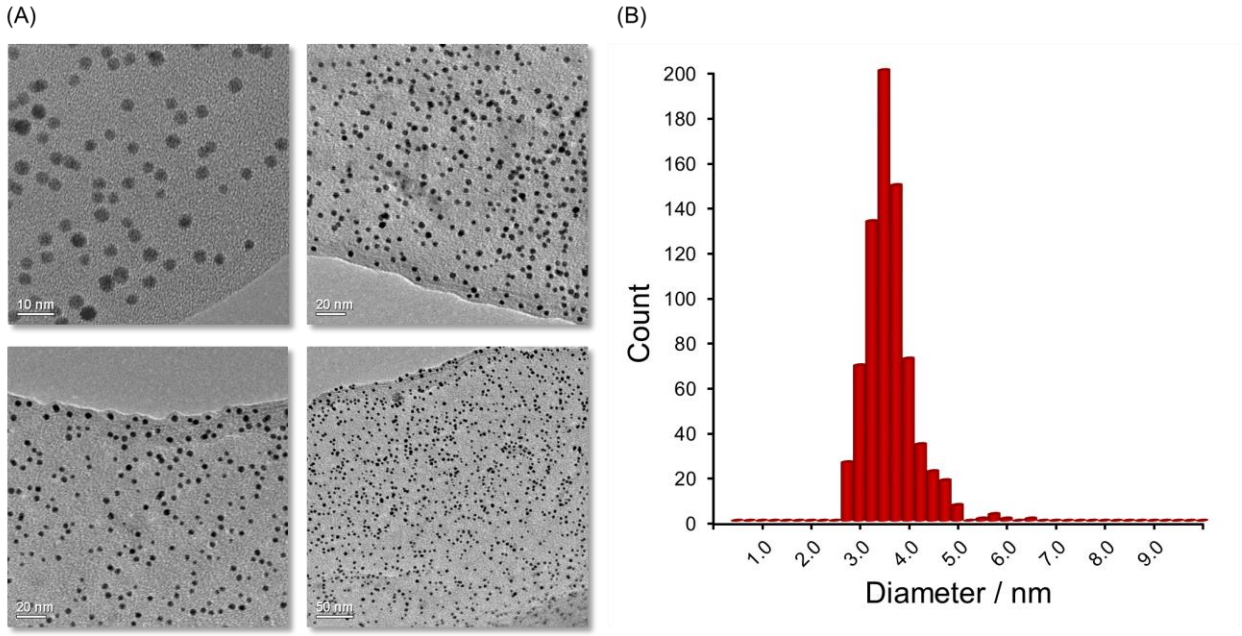

Figure S4 (**A**) Representative TEM images of AuNP-**S3** and (**B**) histogram of NP size distribution as found through analysis of several images using ImageJ software, as described in the general methods section. AuNP-**S3** were found to have a size of 3.48 ± 0.49 nm, corresponding to a dispersity of 14%.

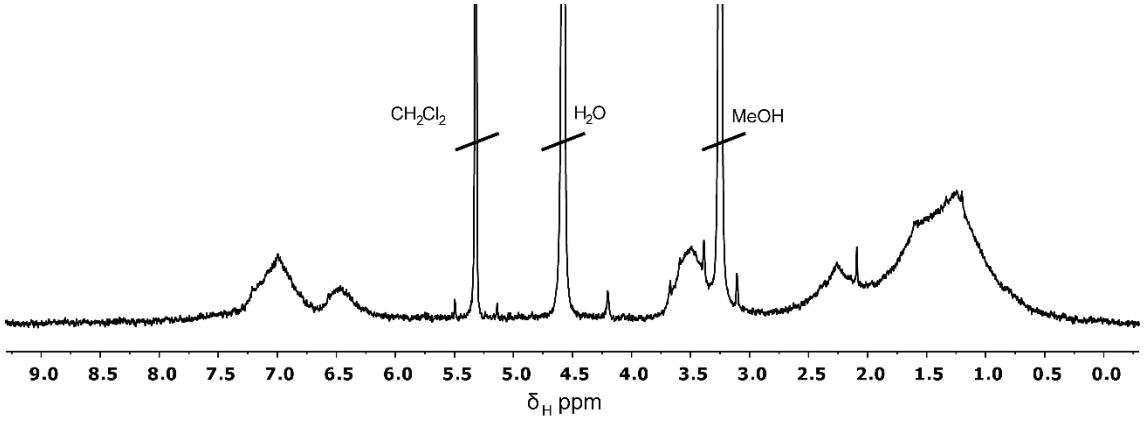

Figure S5 ^{1}H NMR spectrum (CD_2Cl_2/CD_3OD, 99:1 *v*/*v*, 400.1 MHz, 298 K) of AuNP-**2**.

4. NP-bound boronate ester formation and equilibration

4.1 Relaxation time measurements

Spin-lattice relaxation times (T_1) were measured using an inversion recovery method and analysed using Mestrenova 9.0 for the ^{19}F resonance of all relevant species at ca. 5–10 mM in CD_3OD/CD_2Cl_2 (10:1, *v*/*v*) with of *N*-methylmorpholine (≈ 500 mM).

Table S2 Measured T_1 values for all compounds and complexes studied.

Species	T_1 **/s**
3-fluoro-4-bromonitrobenzene **IS**	3.8
3-fluorocatechol **2**	2.1
4-fluorocatechol **4**	2.7
3-fluorocatechol ester [**S4·2**]	1.2
4-fluorocatechol ester [**S4·4**]	1.4
3-fluorocatechol NP-ester AuNP-**3**	1.0
4-fluorocatechol NP-ester AuNP-**5**	0.9

3-Fluoro-4-bromonitrobenzene (used as an internal standard in all quantative ^{19}F NMR experiments) was determined as the slowest relaxing species with T_1 = 3.8 s. As such, a D_1 time of 20 s was employed for obtaining all quantitative ^{19}F NMR experiments.

4.2 Boronate ester response to base concentration

A number of Lewis bases could be used to stabilize NP-bound boronate esters, including *N*-methylmorpholine or *N*,*N*-diisopropylethylamine. The extent of ester formation was found to depend on the concentration of base added. For an equimolar mixture of boronic acid and catechol at 5 mM each, boronate ester formation reached a saturation value of 3.7 mM after addition of 130 mM *N*-methylmorpholine (26 equivalents with respect to boronic acid, **Figure S6**).

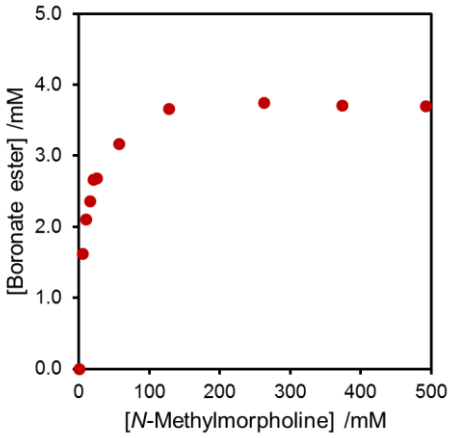

Figure S6 Boronate ester formation as a function of Lewis base concentration as determined by $^{19}F\{^{1}H\}$ NMR spectroscopy (CD_3OD, 275.5 MHz, 298 K). $[\mathbf{S4}]_0$ = 5.0 mM, $[\mathbf{4}]_0$ = 5.0 mM.

Boronate ester formation in protic solvents, and stabilized by Lewis bases, involves a complex set of equilibria describing the relationship between trigonal and tetrahedral boron species, boronic(ate) acids and boronic(ate) esters, and also tetrahedral coordination of boron by either solvent, Lewis base or catechol species (the latter may also be in at least two different protonation states). To ensure consistency across all quantitative NMR experiments, a large excess of base was therefore employed (typically 100 equivalents with respect to boronic acid). This is important, for example, during the experiment reported in **Figure 2** and Section 4.5 below, where it ensures consistent operation of the dynamically adaptable boronate ester monolayer even in the presence of > 2.3 M of acidic catechol species.

It should be noted however, that formation and equilibration of NP-bound boronate esters behaves in precisely the same fashion at much lower concentrations of base, corresponding to < 10 equivalents with respect to boronic acid. See, for example, **Figure S15** and Section 4.4.2.

4.3 Titrations to establish NP-bound boronate ester surface saturation

AuNP-**1** (56.35 mg, 0.0295 mmol in terms of **1**), 4-bromo-3-fluoronitrobenzene internal standard (3.71 mg, 0.0169 mmol) and *N*-methylmorpholine (299 mg, 325 µL) were dissolved in CD_3OD/CD_2Cl_2 (10:1 *v*/*v*, 3.3 mL) to give **Solution A**. 3-Fluorocatechol (16.39 mg, 0.128 mmol) was dissolved in **Solution A** (0.6 mL) to give **Solution 3-F**. 4-Fluorocatechol (16.51 mg, 0.129 mmol) was dissolved in **Solution A** (0.6 mL) to give **Solution 4-F**. The final concentrations were as shown in **Table S3**.

Table S3 Summary of the concentrations in solutions prepared for nanoparticle-bound boronate ester formation.

	Solution A	Solution 3-F	Solution 4-F
AuNP-**1** (in terms of **1**)	8.95 mM	8.95 mM	8.95 mM
3-fluorocatechol **2**	0.00 mM	213.24 mM	0.00 mM
4-fluorocatechol **4**	0.00 mM	0.00 mM	214.81 mM
N-methylmorpholine	895 mM	895 mM	895 mM
Internal standard **IS**	5.11 mM	5.11 mM	5.11 mM

Solution 3-F or **4-F** was titrated into **Solution A**. After each addition, the resulting solution was analysed by $^{19}F\{^1H\}$ NMR spectroscopy (**Figure S7**, CD_3OD/CD_2Cl_2 10:1 *v*/*v*, 275.5 MHz, 298 K, D_1 = 20 s, ns = 16)

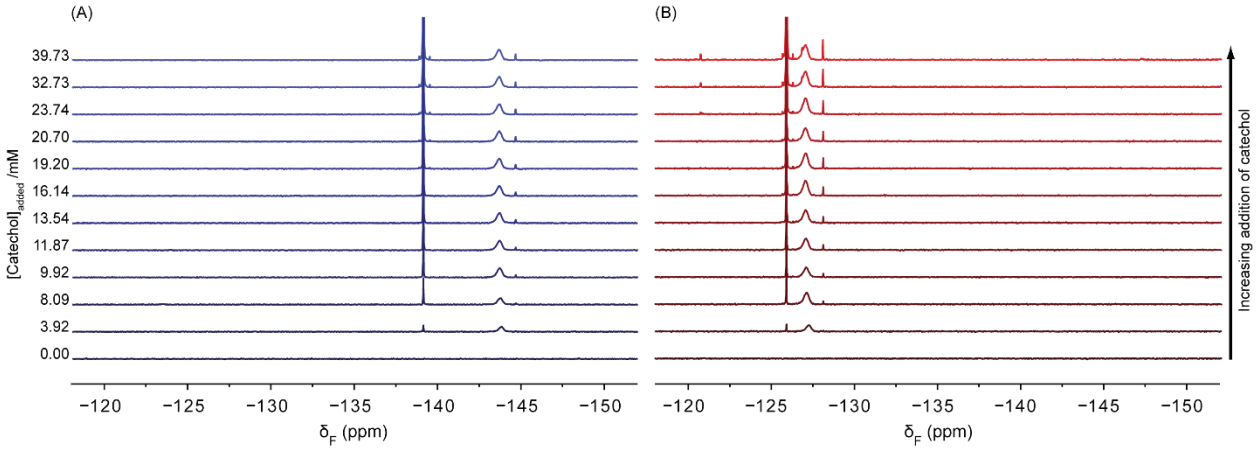

Figure S7 Partial $^{19}F\{^1H\}$ NMR spectra (CD_3OD/CD_2Cl_2 10:1 *v*/*v*, 275.5 MHz, 298 K) of titrations of AuNP-**1** with (**A**) 3-fluorocatechol **2** and (**B**) 4-fluorocatechol **4** in the presence of *N*-methylmorpholine (900 mM).

The broad signal for nanoparticle-bound boronate esters **3** and **5** was integrated relative to the internal standard to determine the fraction of boronic acids converted to boronate esters. The concentration of boronate esters is expressed as a fraction of the total boronic acid concentration as determined by ICP-OES and plotted as a function of total added catechol in **Figure S8**.

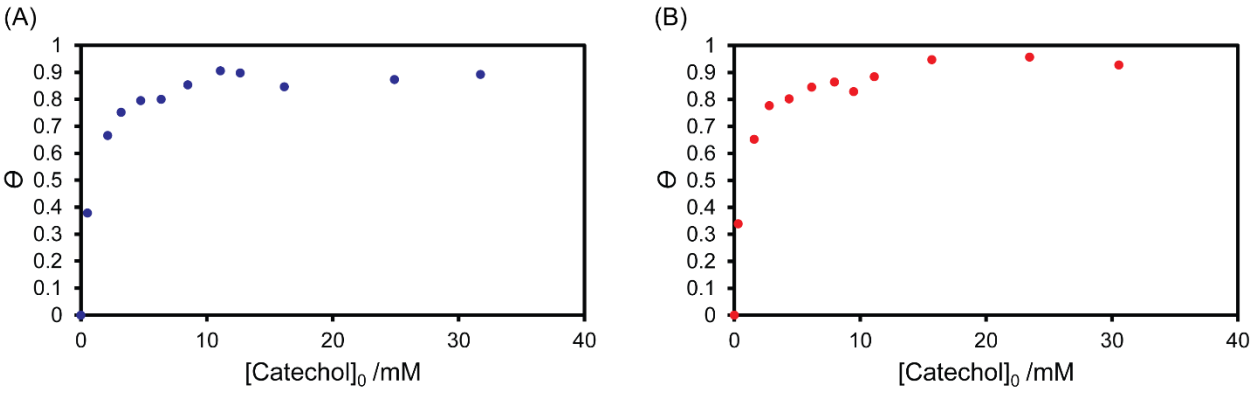

Figure S8 Titration curves for titrations of AuNP-**1** with (**A**) 3-fluorocatechol **2** and (**B**) 4-fluorocatechol **4** in CD_3OD/CD_2Cl_2 10:1 *v*/*v* with 900 mM *N*-methylmorpholine.

4.3.1 Nanoparticle-bound boronate ester modelling

We reason that the < 100% saturation of the available boronic acids can be largely ascribed to steric and/or electrostatic repulsion. By simply approximating the nanoparticle-bound ligand as a cone, the diameter at the base of the cone can be calculated[S2] (**Figure S9**).

The nanoparticle radius (A1) was determined from TEM images as 1.71 nm (**Figure S1**), and the maximum ligand length estimated by modelling its extended conformation (**Figure S10**). X1 can be approximated as 0.265 nm from the area occupied per ligand, calculated from ICP-OES data (**Table S1**) as 0.220 nm^2 (in good agreement with values reported in the literature[S3]).

Θ can therefore be calculated as 8.81°. A (= A1 + A2) = 3.86 nm. Therefore D can be calculated as 1.20 nm.

This crude model makes a number of assumptions. The nanoparticles are assumed to be monodisperse, and spherical. The nanoparticle surface area occupied by a ligand is approximated as a circle and the ligand is assumed to be fully extended.

Nevertheless, the modelled diameter of the boronate ester complex (0.95 nm, **Figure S11**) is only very slightly smaller than the volume available at the periphery of the monolayer, which is therefore consistent with high, but < 100% surface saturation concentrations.

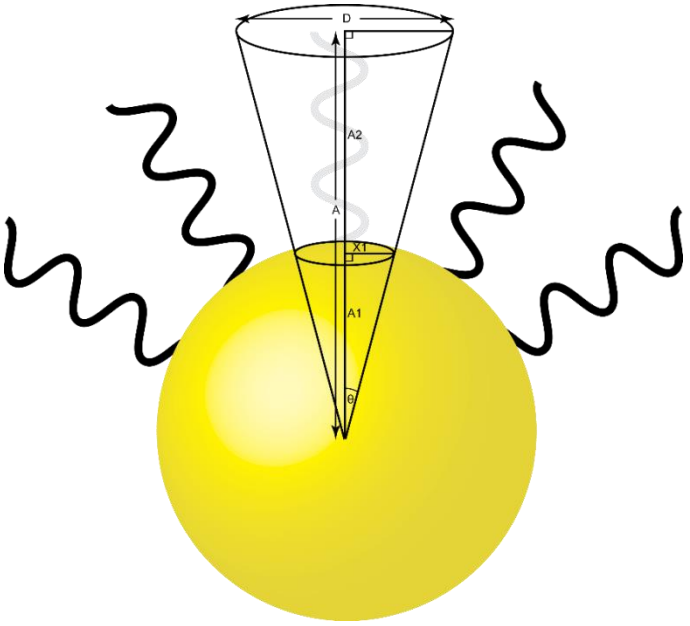

Figure S9 Simple geometric model of the cone volume occupied by a ligand. *D* is the diameter at the boronic acid of the ligand, and approximates the space available for binding.

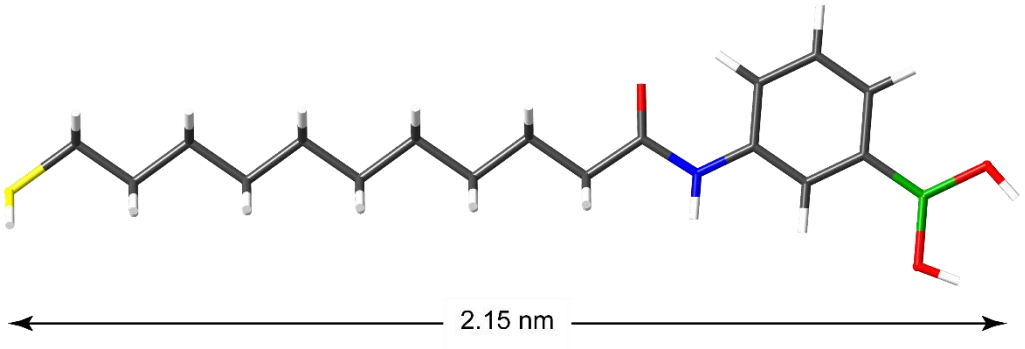

Figure S10 Extended model of nanoparticle-bound boronic ester ligand (Maestro 2012). The sulfur–oxygen distance was measured as 2.15 nm.

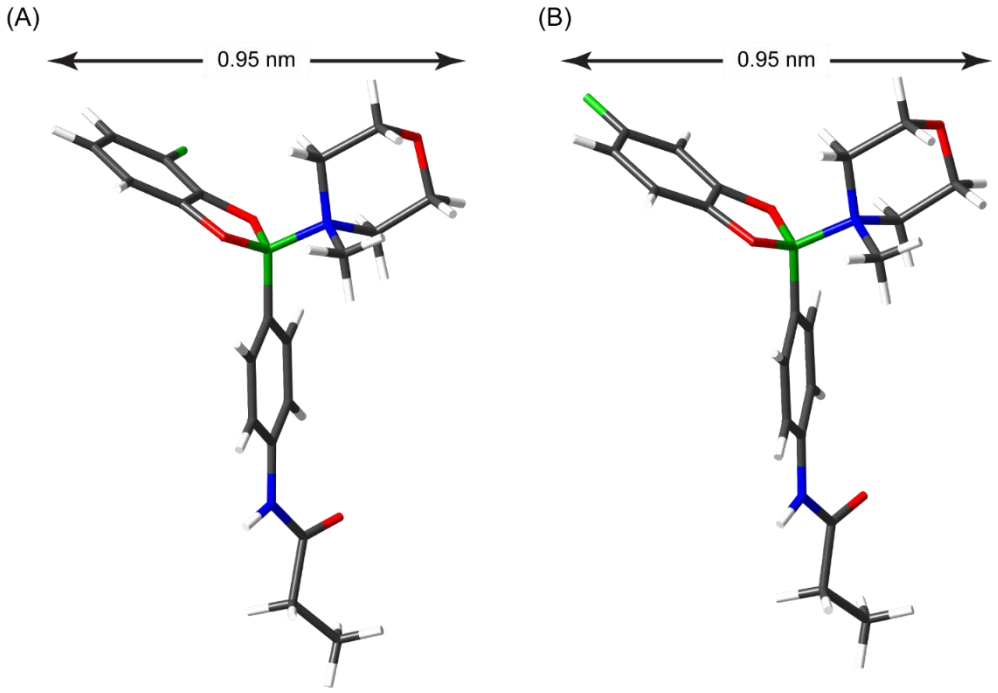

Figure S11 Stick representation of the minimised structure (Maestro 2012, MMFF/GB/SA octanol solvation) of model boronic ester formed with (**A**) 3-fluorocatechol **2** and (**B**) 4-fluorocatechol **4**. The longest distance measured across the complex is 0.95 nm in each case.

4.4 Approaching equilibrium via different pathways

4.4.1 NP-Bound boronate ester equilibration at high Lewis base concentration

Solution A, **Solution 3-F**, and **Solution 4-F** were prepared as described in Section 4.3 The spectra reported in **Figures 1**, **S12A**, **S13A** and **S14** were generated as follows. To two separate samples of **Solution A** (2 × 500 µL) was added **Solution 3-F** or **Solution 4-F** (70 µL) and $^{19}F\{^{1}H\}$ NMR spectra of each sample were obtained. A further 70 µL of the alternate **Solution 3-F**/**4-F** was added to the appropriate sample and $^{19}F\{^{1}H\}$ NMR spectra of each sample were obtained again.

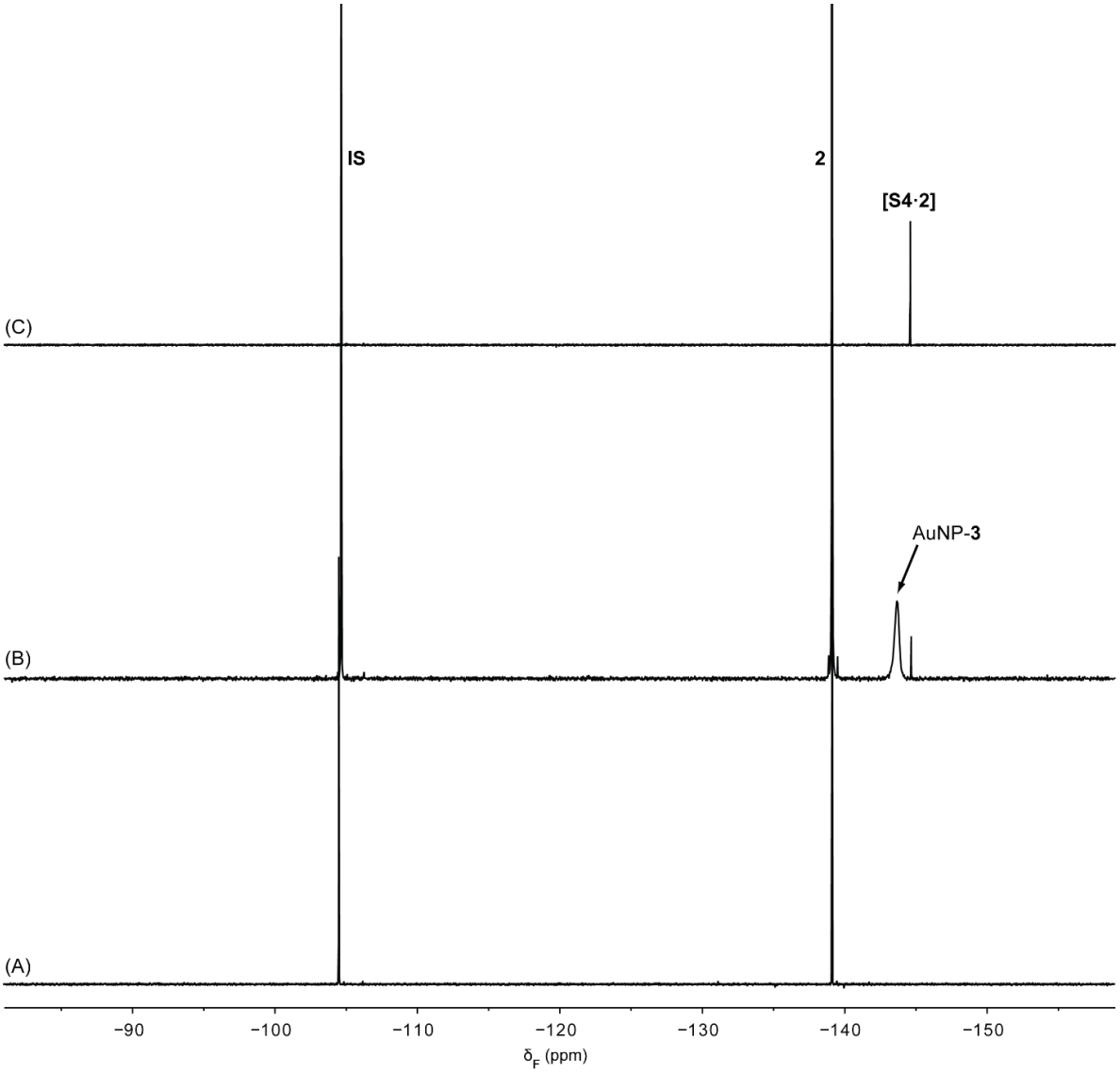

Figure S12 Full sweep width $^{19}F\{^{1}H\}$ NMR spectra (CD_3OD/CD_2Cl_2 10:1 *v*/*v*, 275.5 MHz, 298 K) of boronic esters formed in the presence of *N*-methylmopholine (900 mM) with 3-fluorocatechol **2** and (**A**) AuNP-**1** prior to the addition of base, (**B**) AuNP-**1** (to give boronate ester **3**) and (**C**) model compound **S4** to give a molecular analogue.

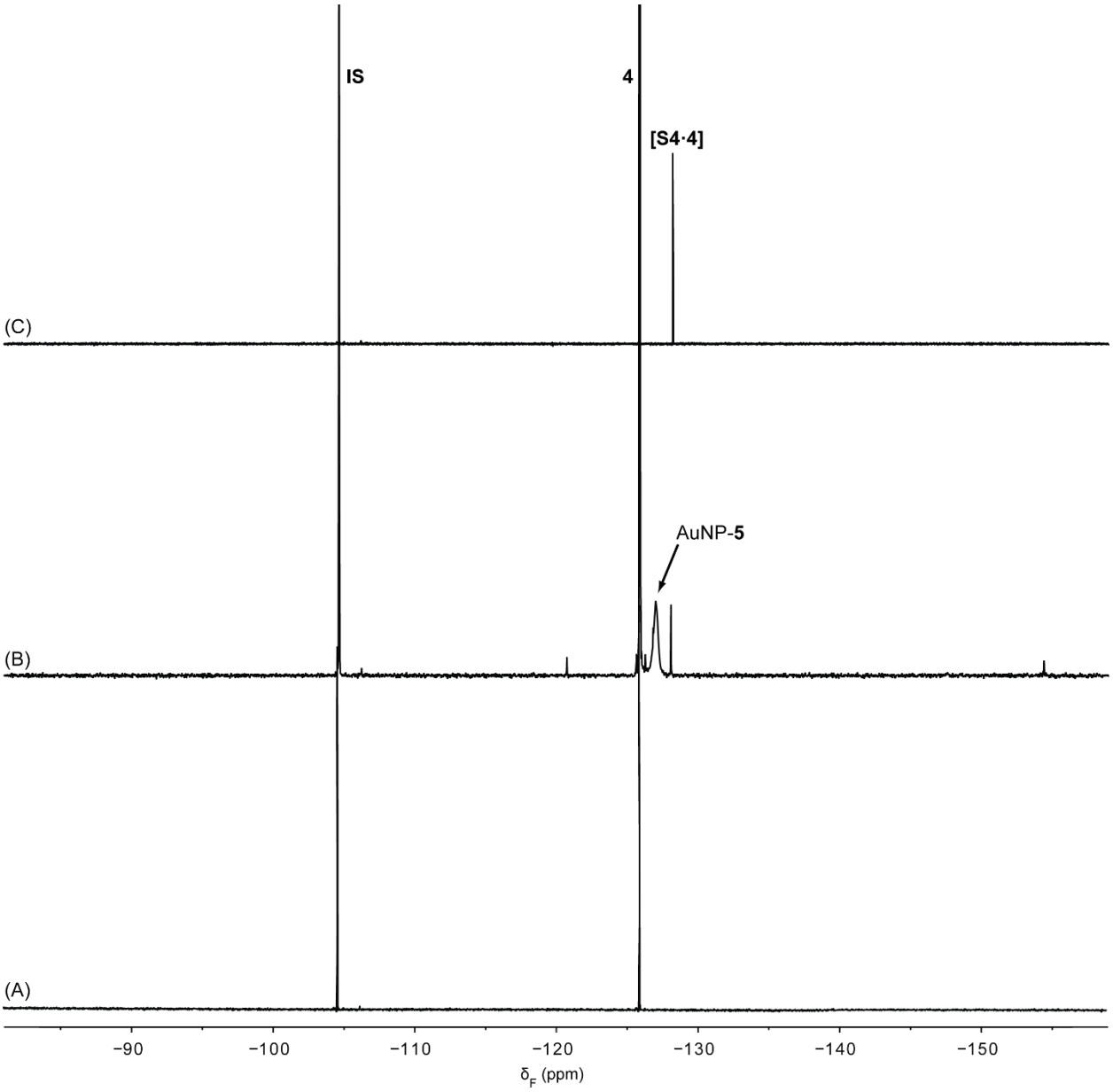

Figure S13 Full sweep width $^{19}F\{^{1}H\}$ NMR spectra (CD_3OD/CD_2Cl_2 10:1 *v*/*v*, 275.5 MHz, 298 K) of boronic esters formed in the presence of *N*-methylmopholine (900 mM) with 4-fluorocatechol **4** and (**A**) AuNP-**1** prior to the addition of base, (**B**) AuNP-**1** (to give boronate ester **5**) and (**C**) model compound **S4** to give a molecular analogue.

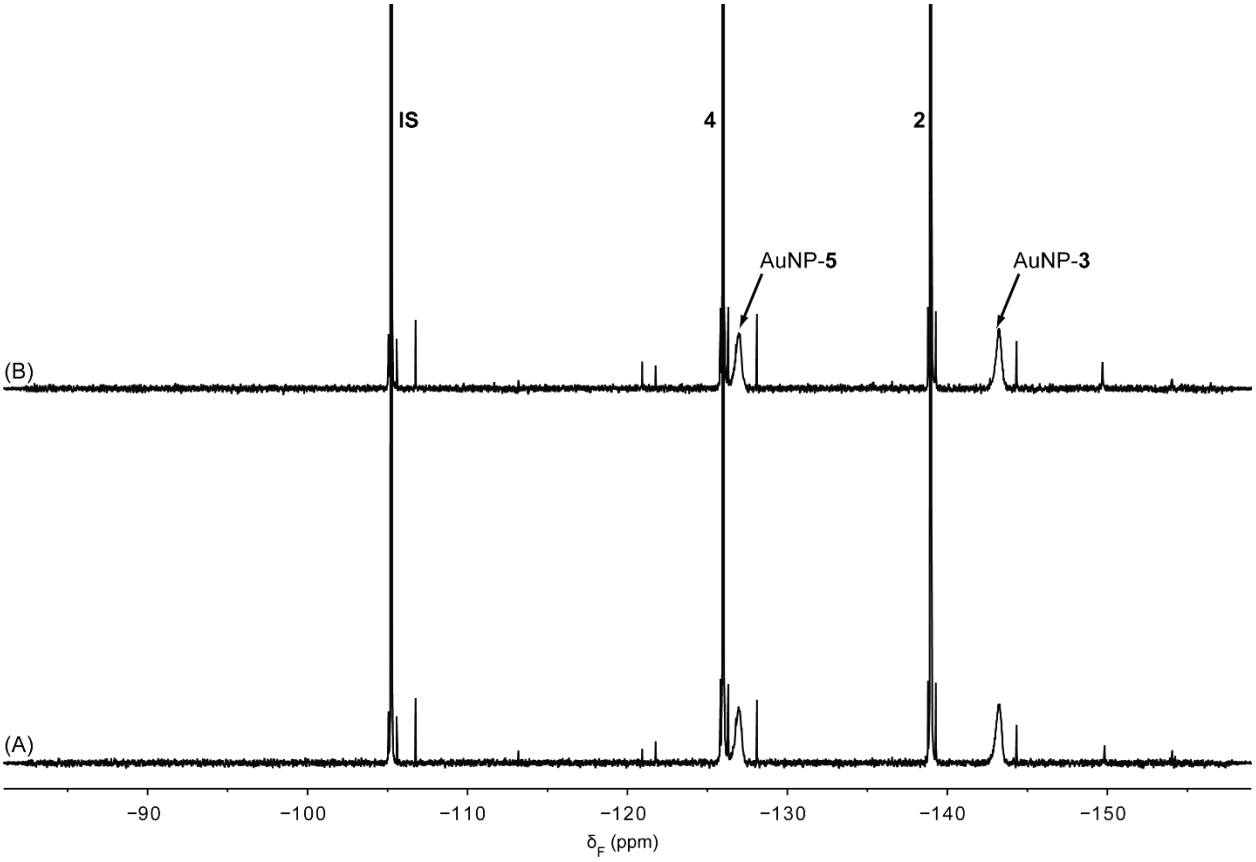

Figure S14 Full sweep width $^{19}F\{^{1}H\}$ NMR spectra (CD_3OD/CD_2Cl_2 10:1 *v*/*v*, 275.5 MHz, 298 K) corresponding to **Figure 1d**.

Initial concentrations: (both traces) [AuNP-**1**]$_0$ = 9.0 mM, [**2**]$_0$ = 26 mM, [**4**]$_0$ = 26 mM, [*N*-methylmorpholine] = 900 mM.

Equilibrium concentrations: (top trace) [**3**] = 3.8 mM, [**4**] = 3.7 mM; . (bottom trace) [**3**] = 3.8 mM, [**4**] = 3.7 mM.

4.4.2 NP-Bound boronate ester equilibration at low Lewis base concentration

The experiment described in Section 4.4.1 and reported in **Figures 1**, **S12–S14** was repeated for a AuNP-**1** stock solution at 10 mM (in terms of **1**) and using *N*,*N*-diisopropylethylamine as Lewis base at 70 mM (7 equivalents with respect to **1**). Precisely the same thermodynamically controlled equilibration behaviour was observed (**Figure S15**).

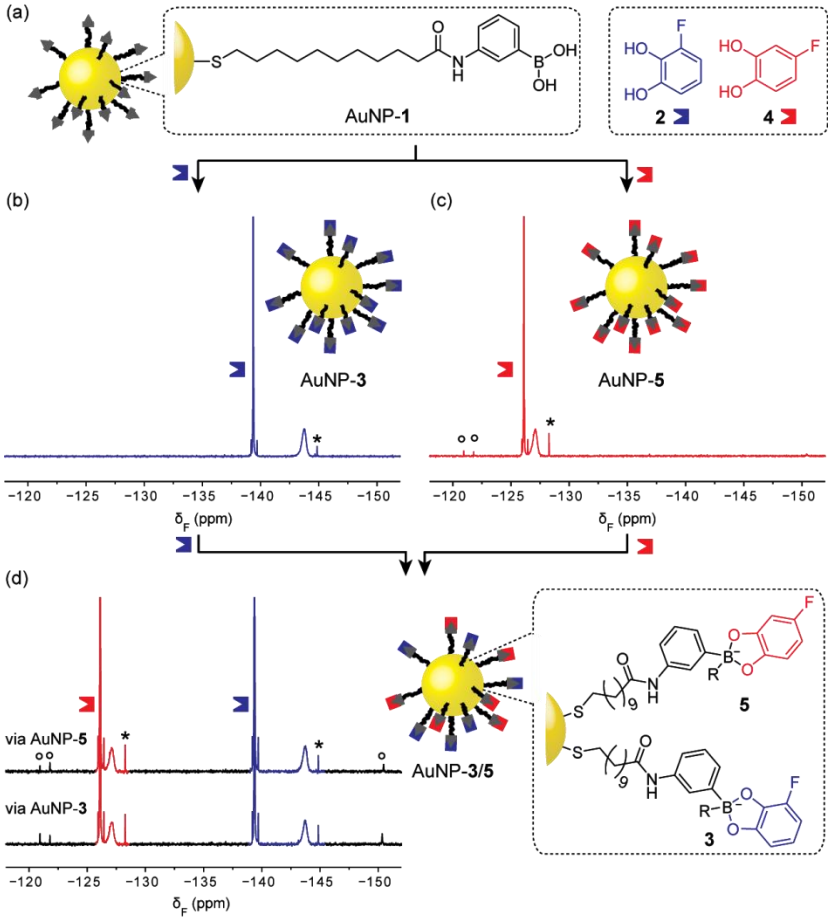

Figure S15 NP-Bound boronate ester formation and dynamic covalent exchange at low Lewis base concentration: [*N*,*N*-diisopropylethylamine] = 70 mM. (a) Structure of AuNP-**1**, catechols **2** and **4**. (b,c,d) Partial $^{19}F\{^{1}H\}$ NMR spectra (CD_3OD/CD_2Cl_2, 10:1 *v*/*v*, 470.5 MHz, 298 K) indicating NP-bound boronate ester formation in the presence of: (b) an excess of catechol **2**; (c) an excess of catechol **4**. (d) Identical mixed monolayer compositions of NP-bound boronate esters **3** and **5** prepared from either surface saturated AuNP-**3** (bottom trace) or AuNP-**5** (top trace).
Initial concentrations: (b) [AuNP-**1**]$_0$ = 10.0 mM, [**2**]$_0$ = 39 mM, [**4**]$_0$ = 0.0 mM; (c) [AuNP-**1**]$_0$ = 10.0 mM, [**2**]$_0$ = 0.0 mM, [**4**]$_0$ = 36 mM; (d, both traces) [AuNP-**1**]$_0$ = 10.0 mM, [**2**]$_0$ = 39 mM, [**4**]$_0$ = 39 mM. All experiments: [*N*,*N*-diisopropylethylamine]$_0$ = 70 mM
Equilibrium concentrations: (b) [AuNP-**3**] = 8.9 mM; (c) [AuNP-**4**] = 8.2 mM; (d, top trace) [**3**] = 4.2 mM, [**4**] = 3.9 mM; . (d, bottom trace) [**3**] = 4.1 mM, [**4**] = 4.0 mM.
Signals marked * correspond to desorbed ligand, which appears slowly in the presence of base; signals marked ° arise from oxidative decomposition of **4**. The sum of all impurities amounts to < 4% of total fluorine-containing species.

4.5 Cyclable boronate ester equilibration

AuNP-**1** (8.90 mg, 0.00467 mmol in terms of **1**), 4-bromo-3-fluoronitrobenzene (internal standard **IS**, 2.46 mg, 0.0112 mmol) and *N*-methylmorpholine (49 mg, 53 µL, 0.484 mmol) were dissolved in CD_3OD/CD_2Cl_2 (10:1 *v*/*v*, 520 µL) to give a solution containing 9.0 mM AuNP-**1** (in terms of **1**). 3-fluorocatechol (**2**) was added as a solid, and the solution was analysed by $^{19}F\{^1H\}$ NMR spectroscopy (**Figure S16**, CD_3OD/CD_2Cl_2 10:1 *v*/*v*, 275.5 MHz, 298 K). The concentrations of catechol **2** and nanoparticle-bound boronate ester **3** were determined by integration relative to the internal standard. After each subsequent addition of **2** or 4-fluorocatechol (**4**), the solution was again analysed again by $^{19}F\{^1H\}$ NMR spectroscopy (**Figure S16**, CD_3OD/CD_2Cl_2 10:1 *v*/*v*, 275.5 MHz, 298 K). Concentrations of catechols **2** and **4** and boronate esters **3** and **5** were determined by integration relative to the internal standard (**Figure 2**).

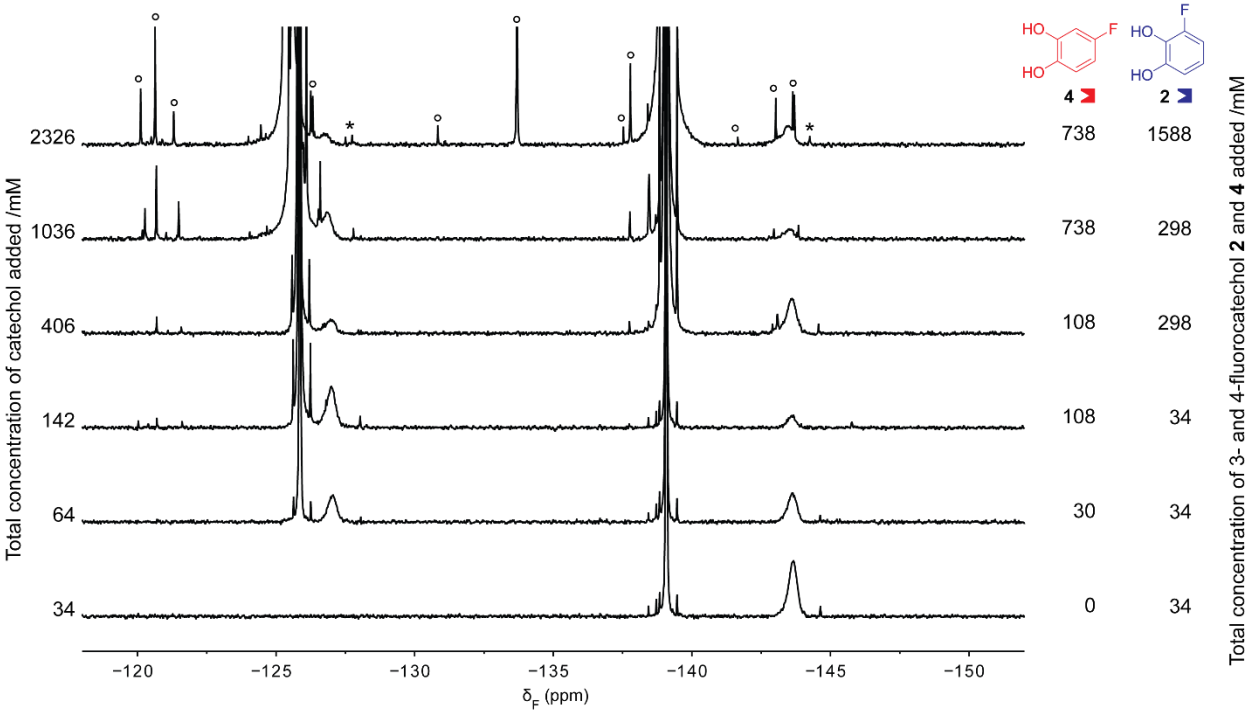

Figure S16 Partial $^{19}F\{^1H\}$ NMR spectra (CD_3OD/CD_2Cl_2 10:1 *v*/*v*, 275.5 MHz, 298 K) of successive alternating additions of 3-fluorocatechol **2** and 4-fluorocatechol **4** to AuNP-**1** (9.0 mM in terms of **1**) in the presence of *N*-methylmorpholine (900 mM). Signals marked * correspond to desorbed ligand, which appears slowly in the presence of base; signals marked ° arise from impurities present in and oxidative decomposition of **2** and **4**.

5. Nanoparticle assembly

5.1 Assembly with linker 6 or 7

AuNP-**1** (0.1 mg mL^{-1} in MeOH/CH_2Cl_2/*N*-methylmorpholine 90:9:1 *v*/*v*, ca. 40 μM in terms of **1**, 2 mL) was mixed with a solution of linker **6** or **7** (10 μL mL^{-1}, 91 mM in MeOH/CH_2Cl_2/*N*-methylmorpholine 90:9:1 *v*/*v*, 50 μL) in a vial, to give a final concentration of **1** (0.036 mM), linker (0.55 mM) and Lewis base (105 mM). The assembly process was monitored directly by UV-Vis spectroscopy without further dilution. Although no shift in NP plasmon resonance was observed (see below), the aggregation process could be followed by the decrease in UV-Vis extinction as a result of NP precipitation (**Figure S17**). Once the sample had fully precipitated (5 days, **Figure S18B**), the sample was sonicated, producing an unstable suspension, a drop of which was spotted onto a TEM grid and allowed to dry under ambient conditions prior to analysis (**Figures 4a**, **4c**, **S22**, **S21**, **S22**).

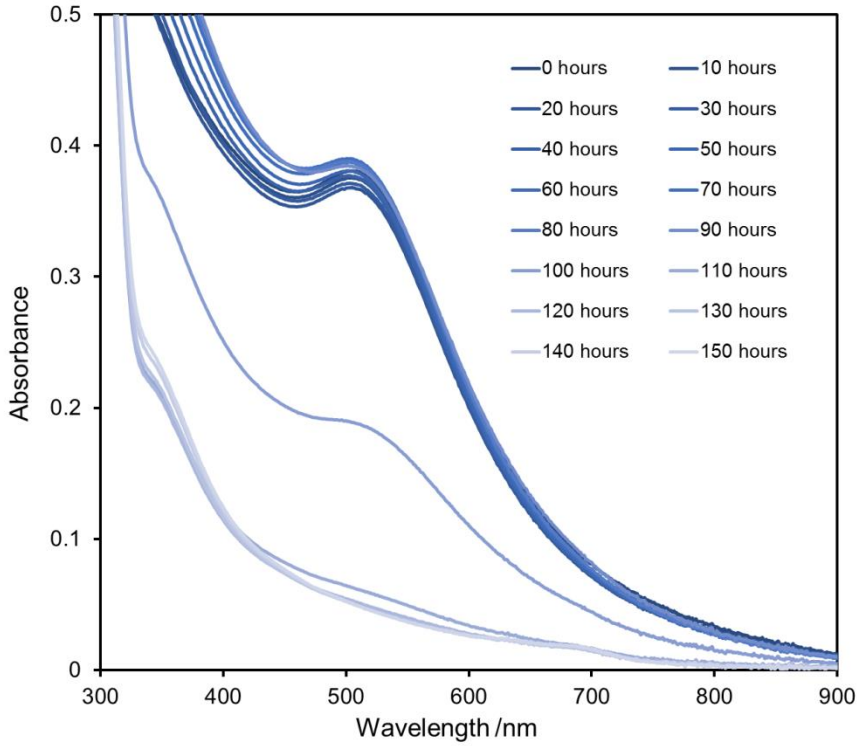

Figure S17 Time course UV-Vis spectra tracking the assembly of AuNP-**1** (0.1 mg mL^{-1}, MeOH/CH_2Cl_2/*N*-methylmorpholine 90:9:1 *v*/*v*, 298 K) in the presence of bis-catechol **6** (0.55 mM).

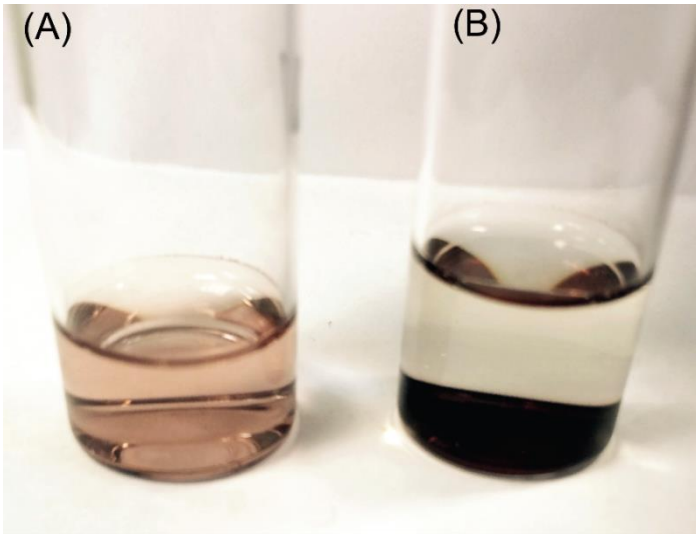

Figure S18 Photograph showing colloidal dispersions of AuNP-**1** (0.1 mg mL^{-1}) in MeOH/CH_2Cl_2 (10:1 *v*/*v*) containing *N*-methylmorpholine (1% *v*/*v*, 105 mM) after 28 days in the absence (**A**) and the presence (**B**) of linker **6** (0.55 mM).

At no stage during the assembly process was a shift in the LSPR band observed by UV-Vis. This is not unexpected for relatively small NPs connected by molecular linkers of similar magnitude in length to the particle size. For a pair of interacting NPs, the decay in plasmon coupling with increasing interparticle distance leads to an exponential decrease in the fractional redshift in LSPR wavelength, with a universal decay length ≈ 0.2 × d, where d is the NP diameter.[S4] In practical terms, this means that redshifts are generally only observable when the interparticle distance is smaller than 0.5 × d.[S5]

In the current example, the interparticle spacing can be crudely estimated as 6.1 nm from the sulfur–sulfur distance in an extended model of the bis(boronate ester) linking unit constructed from **6** and two copies of **1** (**Figure S19**). Thus, the interparticle spacing is roughly 9× the characteristic decay length for NPs with d = 3.4 nm and so it is unsurprising that a redshift is not observed prior to aggregate precipitation from solution.

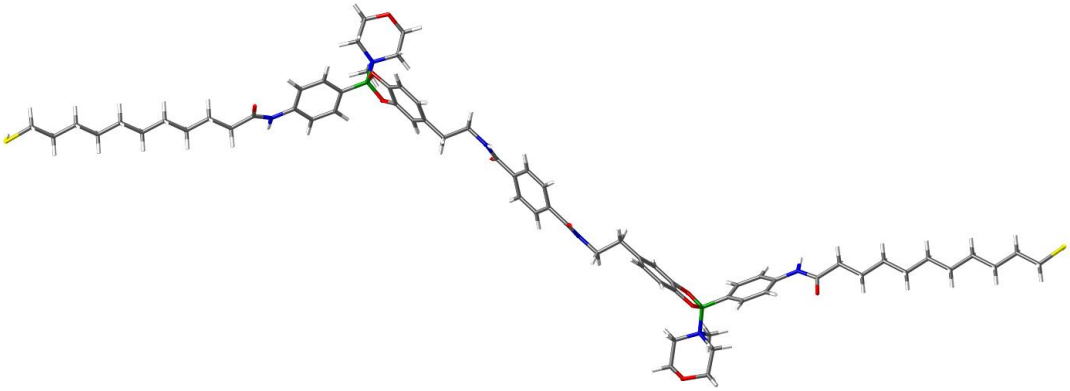

Figure S19 Extended model of nanoparticle-bound boronate ester linkage (Maestro 2012). The sulfur–sulfur distance was measured as 6.09 nm. This is approximately 2 × the NP diameter, and is therefore not expected to produce an observable redshift.[S4,S5]

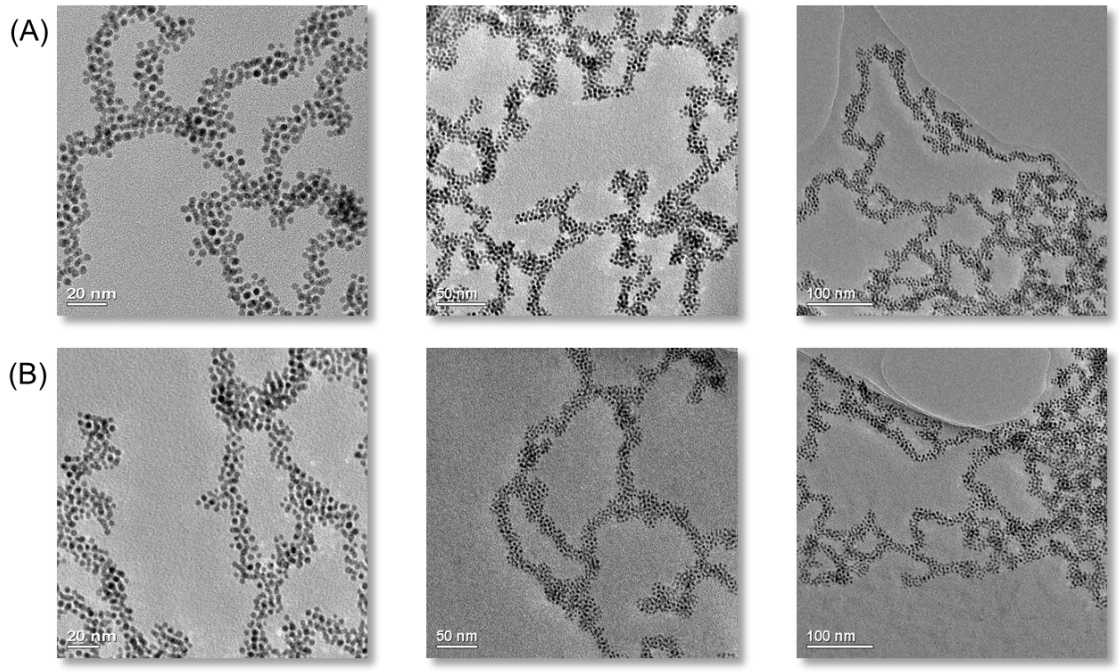

Figure S20 TEM images of aggregates obtained on mixing AuNP-**1** (0.036 mM in terms of **1**), linker **6** (0.55 mM, 15.3 eq.) and *N*-methylmorpholine (105 mM, 2692 eq.) in MeOH/CH_2Cl_2 (10:1 *v*/*v*). Images were obtained from two independently assembled batches (**A**) and (**B**), and show areas of the grid where the chains of nanoparticles can be seen to lie flat on the grid in a single layer, allowing structure visualisation, which reveals a branched-dendritic, net-like assembly.

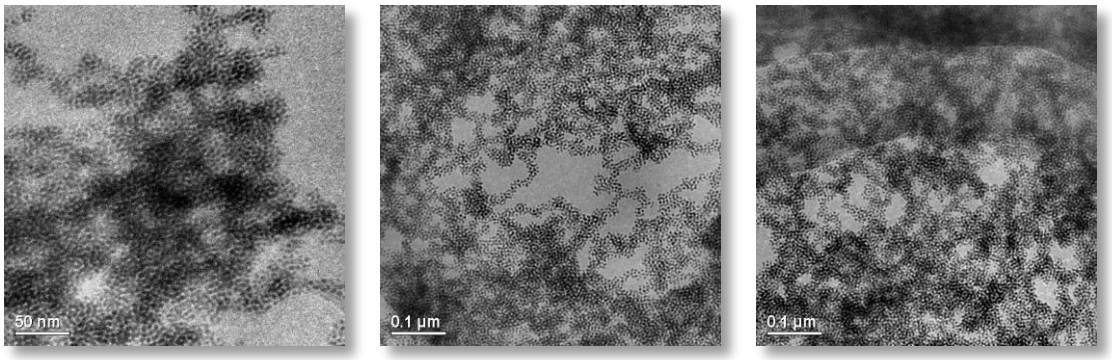

Figure S21 TEM images of aggregates: AuNP-**1** (0.036 mM in terms of **1**), linker **6** (0.55 mM, 15.3 eq.) and *N*-methylmorpholine (105 mM, 2692 eq.) in MeOH/CH_2Cl_2 (10:1 *v*/*v*). These TEM images show the areas where aggregates several layers deep are deposited. The right-hand picture in particular shows that the same net-like structure (seen at the edge of aggregates in the TEM images in **Figure S20**) extends through the entire aggregate.

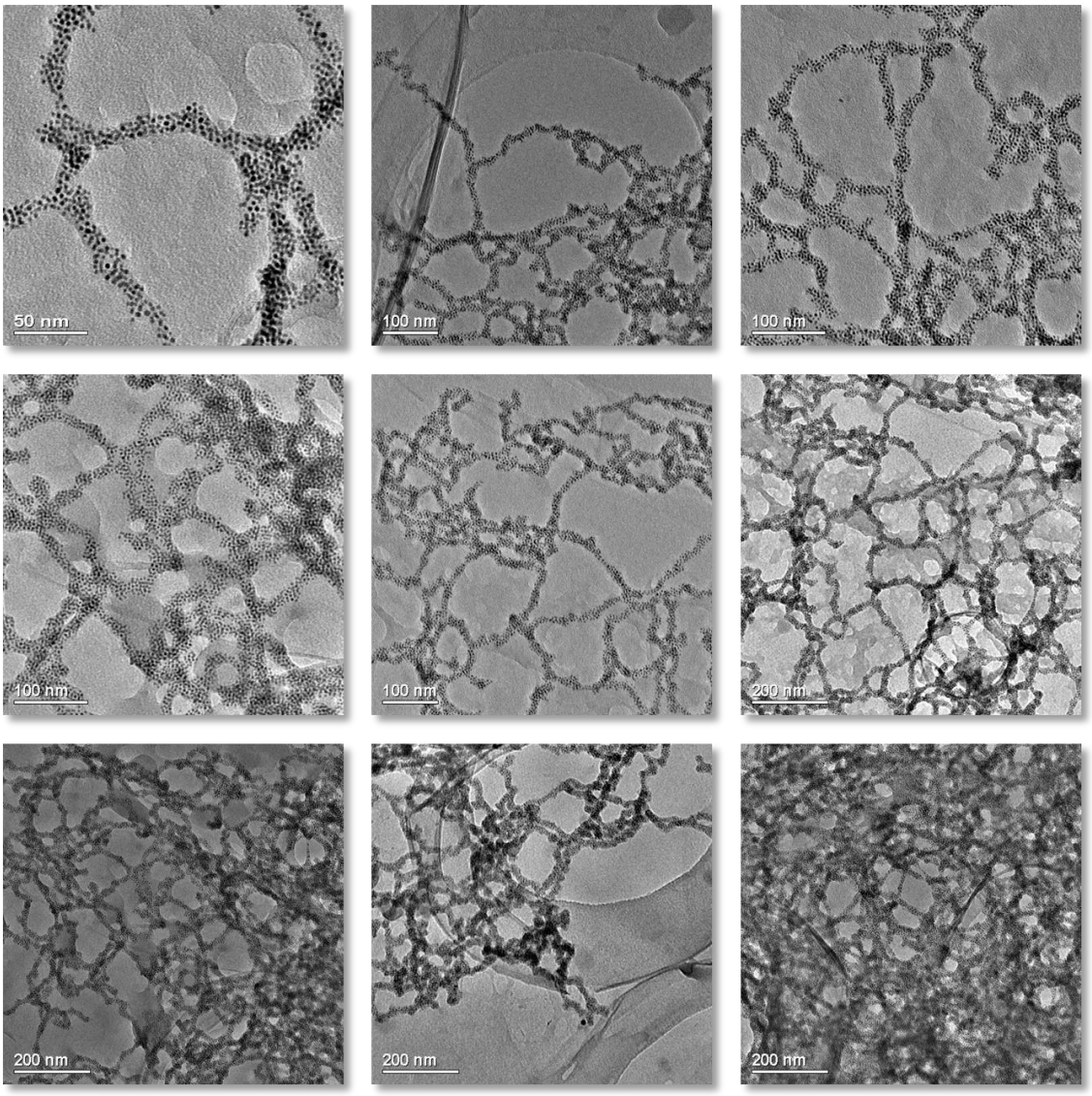

Figure S22 TEM images of aggregates obtained on mixing AuNP-**1** (0.036 mM in terms of **1**), linker **7** (0.55 mM, 15.3 eq.) and *N*-methylmorpholine (105 mM, 2692 eq.) in MeOH/CH_2Cl_2 (10:1 *v*/*v*).

6.2 Control NP assembly experiments

5.2.1 Stability of AuNP-1

The colloidal stability of AuNP-**1** was determined under the assembly conditions by mixing AuNP-**1** (0.1 mg mL^{-1}, 0.036 mM in terms of **1**) and *N*-methylmorpholine (105 mM, 2692 eq.) in MeOH/CH_2Cl_2 (10:1 *v*/*v*). The solution was monitored by UV-Vis spectroscopy for three weeks (**Figure S23**), during which time no loss of material was observed, indicating the colloidal stability of AuNP-**1** under these conditions.

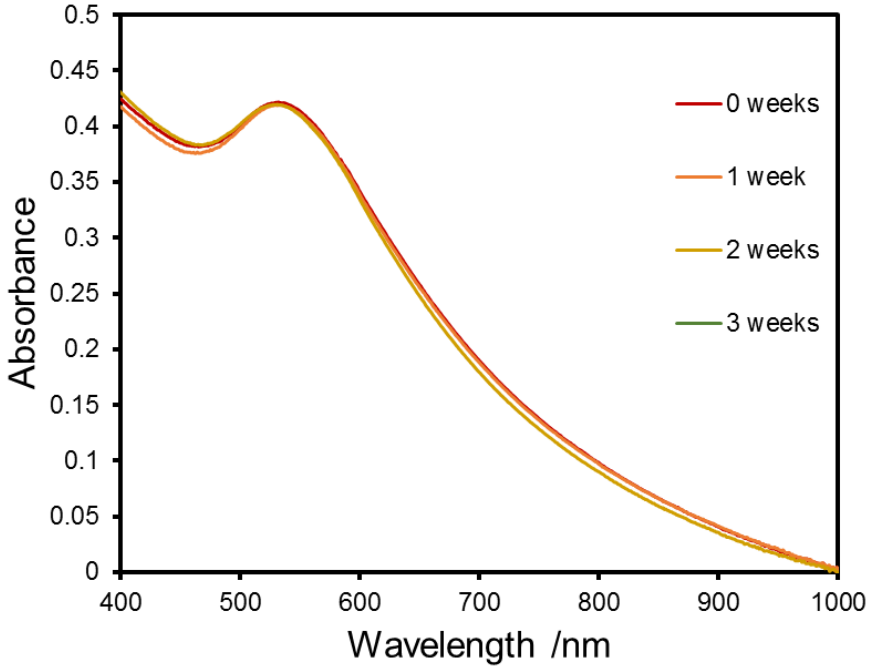

Figure S23 UV-Vis spectra (MeOH/CD_2Cl_2, 10:1 *v*/*v*, 20 °C) showing the colloidal stability of AuNP-**1** (0.1 mg mL^{-1}) in the presence of *N*-methylmorpholine (105 mM, 2692 eq.).

5.2.2 Control AuNP-S3

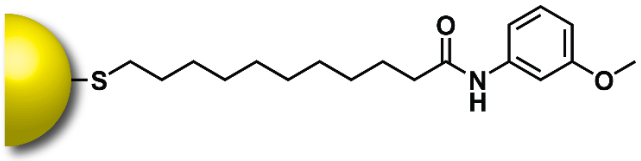

Nanoparticles AuNP-**S3** were synthesized lacking boronic ester functionality in order to rule out non-specific interactions between the linker and the nanoparticle. In a control experiment, AuNP-**S3** (0.1 mg mL^{-1}) was mixed with linker **6** (0.55 mM, 15.3 eq.) and *N*-methylmorpholine (105 mM, 2692 eq.) in $MeOH/CH_2Cl_2$ (10:1 v/v) and allowed to stand for 14 days, during which UV-Vis monitoring of the solution revealed no change in the spectrum (**Figure S24**). The resulting red solution was imaged by TEM (**Figure S25**).

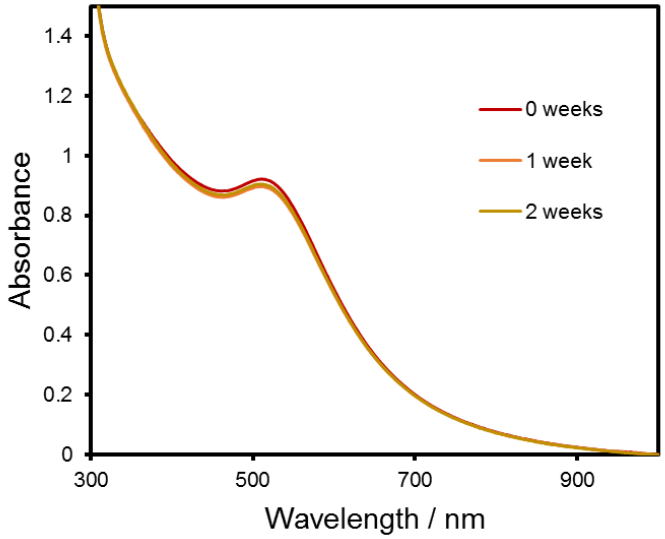

Figure S24 UV-Vis spectra ($MeOH/CD_2Cl_2$, 10:1 *v*/*v*, 20 °C) of AuNP-**S3** (0.1 mg mL^{-1}) linker **6** (0.55 mM, 15.3 eq.) and *N*-methylmorpholine (105 mM, 2692 eq.).

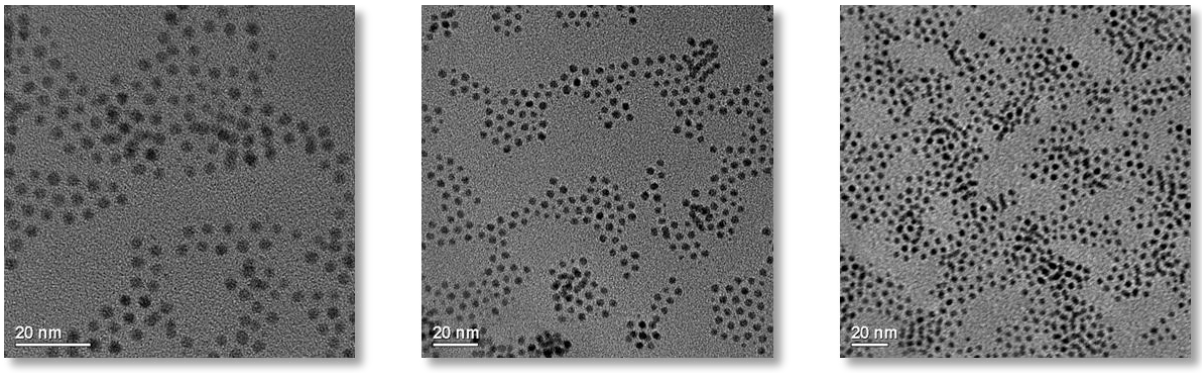

Figure S25 TEM images of a control assembly experiment, obtained 14 days after combining AuNP-**S3** (0.1 mg mL^{-1}), linker **6** (0.55 mM, 15.3 eq.) and *N*-methylmorpholine (105 mM, 2692 eq.) in $MeOH/CH_2Cl_2$ (10:1 *v*/*v*).

5.3 NP Aggregate disassembly

1,2-Dihydroxybenzene (138 mM, 250 eq. relative to **6**) was added to the supernatant of assemblies (prepared as described in Section S5.2). The mixture was non-continuously agitated in an ultrasonic bath for approximately 1 h every day. Upon sonication, a fine red suspension was produced and for the first 30 days, this would settle to produce a black precipitate once agitation ceased. After 35 days, a precipitate no longer formed upon allowing the sample to settle. TEM imaging of the solution at this stage revealed the presence of mostly small spherical assemblies (**Figure S26**), with no large aggregates remaining. After a further 7 days (42 days in total) full disassembly of the nanoparticles was observed (**Figure S27**).

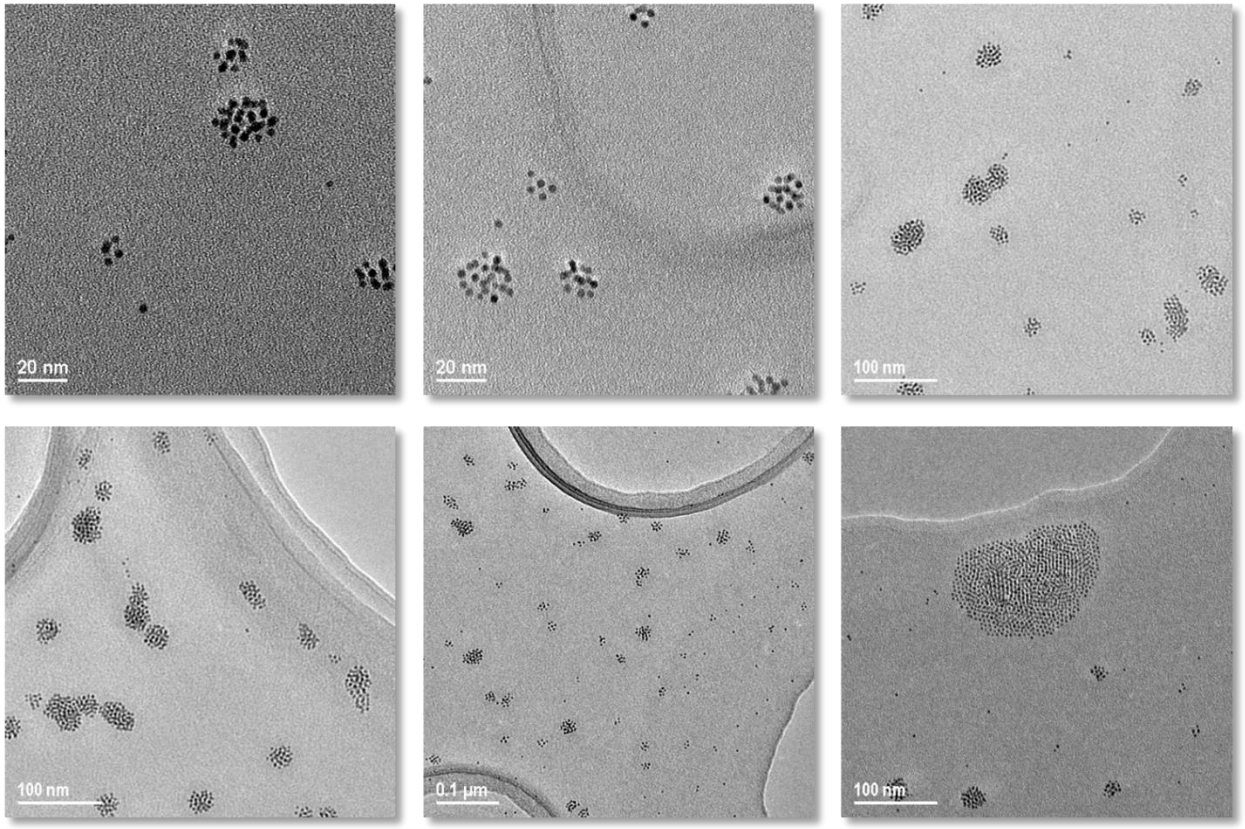

Figure S26 TEM images of partially disassembled aggregates observed 35 days after addition of 1,2-dihydroxybenzene (138 mM, 250 eq. relative to linker) to the supernatant of pre-assembled AuNP-**1**.

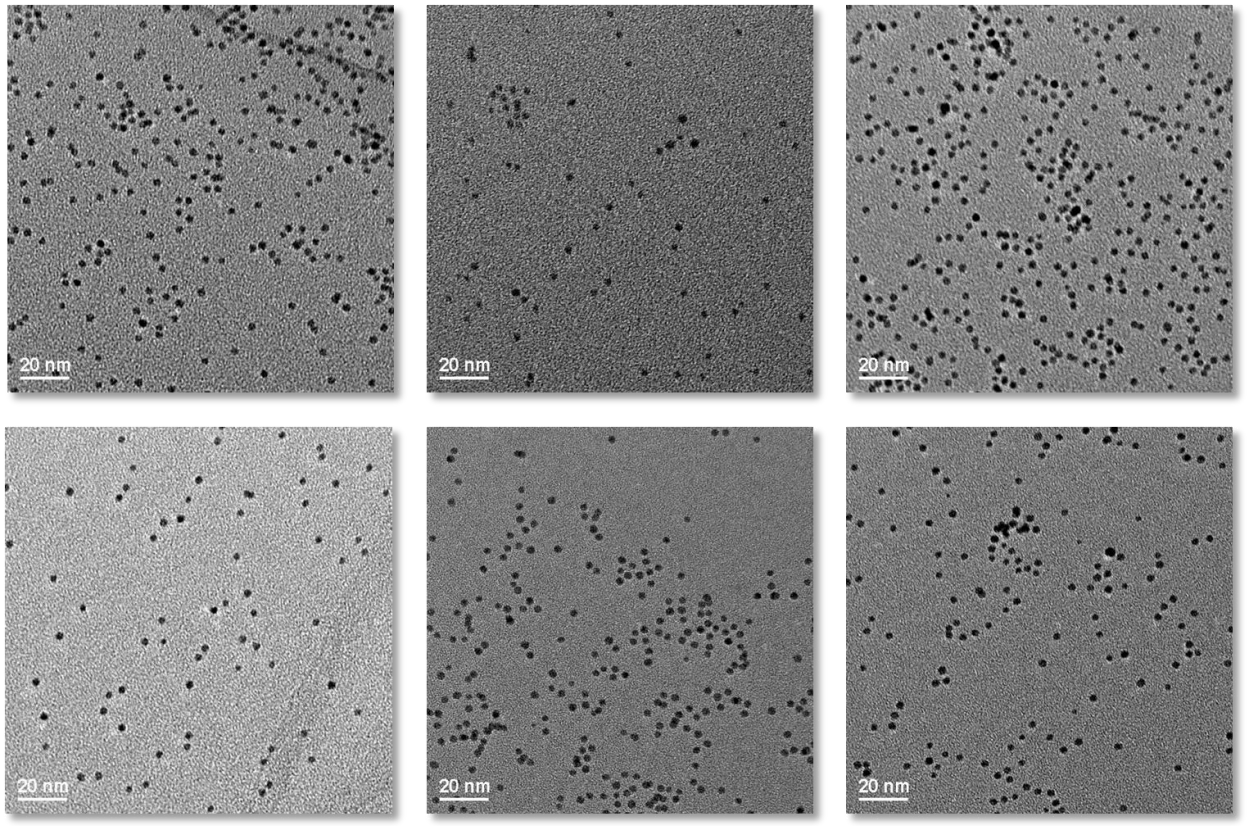

Figure S27 TEM images of quantitatively disassembled aggregates observed 42 days after addition of 1,2-dihydroxybenzene (138 mM, 250 eq. relative to linker) to the supernatant of pre-assembled AuNP-**1**.

7. ^{1}H and ^{13}C NMR spectra of organic compounds

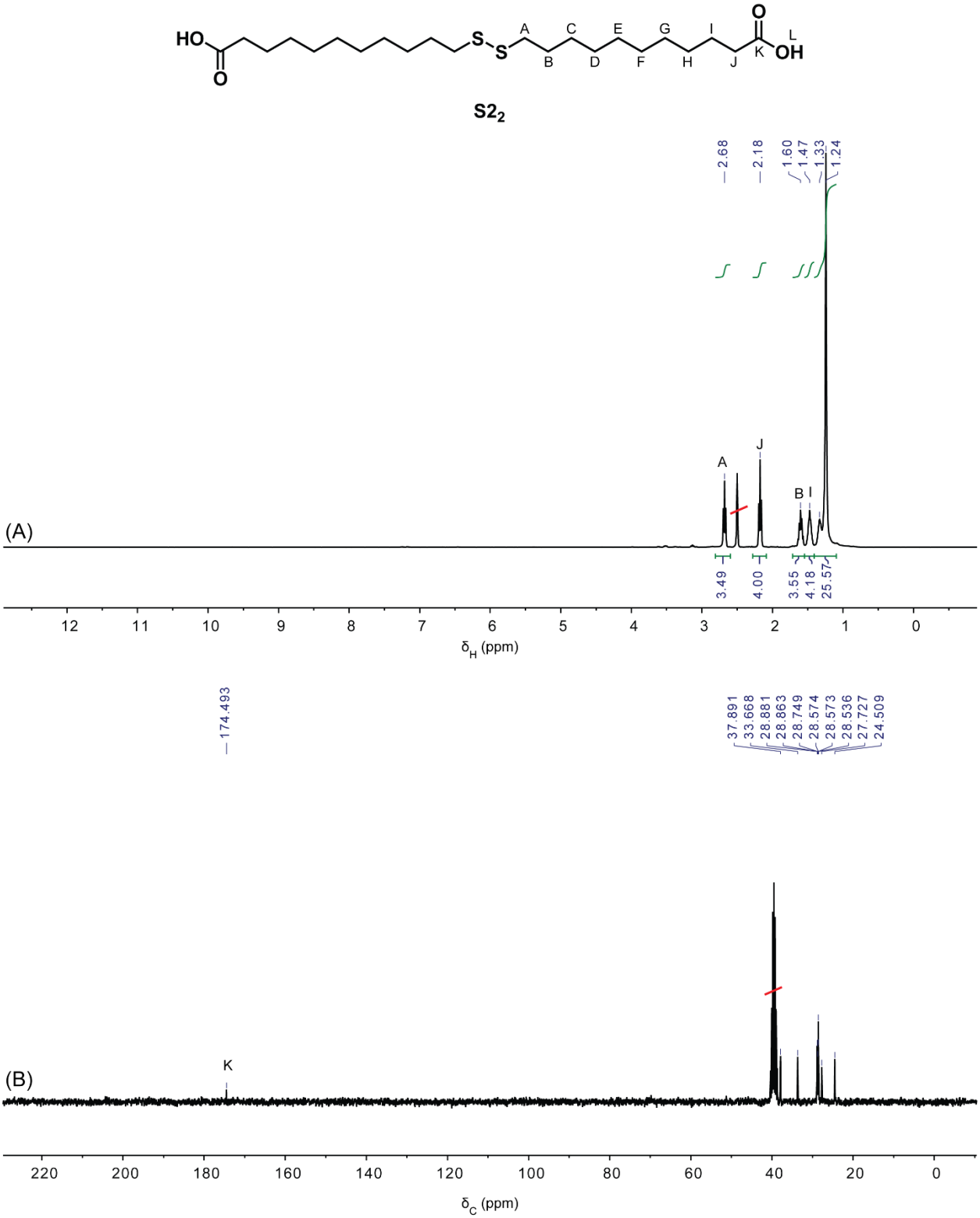

Figure S28 (**A**) ^{1}H NMR spectrum (DMSO-d_6, 300.1 MHz, 298 K) and (**B**) of ^{13}C NMR spectrum (DMSO-d_6, 75.5 MHz, 298 K) of **S2$_2$**.

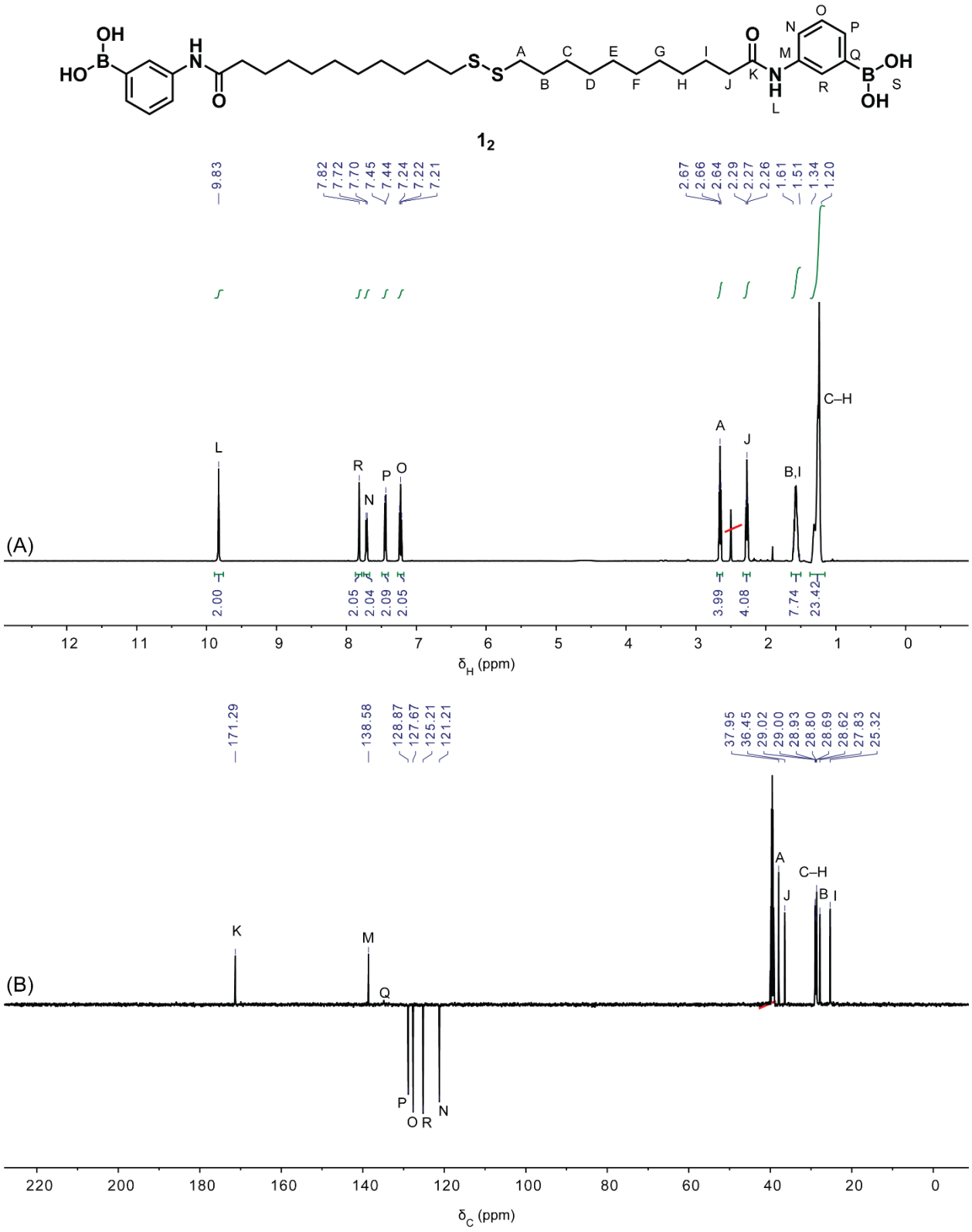

Figure S29 (**A**) ^{1}H NMR spectrum (DMSO-d_6, 500.1 MHz, 298 K) and (**B**) of ^{13}C NMR spectrum (DMSO-d_6, 125.8 MHz, 298 K) of **1_2**.

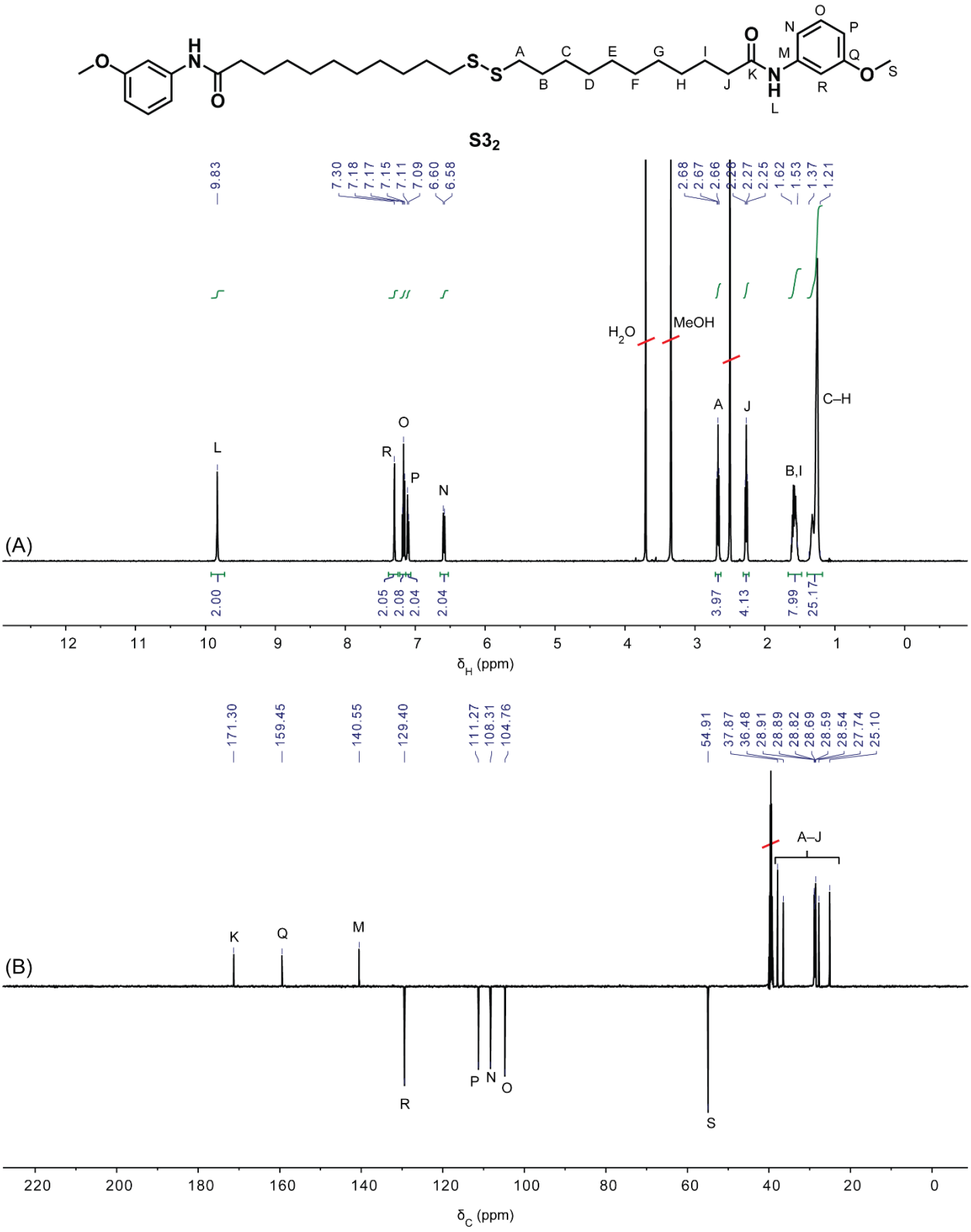

Figure S30 (**A**) ^{1}H NMR spectrum (DMSO-d_6, 500.1 MHz, 298 K) and (**B**) of ^{13}C NMR spectrum (DMSO-d_6, 125.8 MHz, 298 K) of **S3$_2$**.

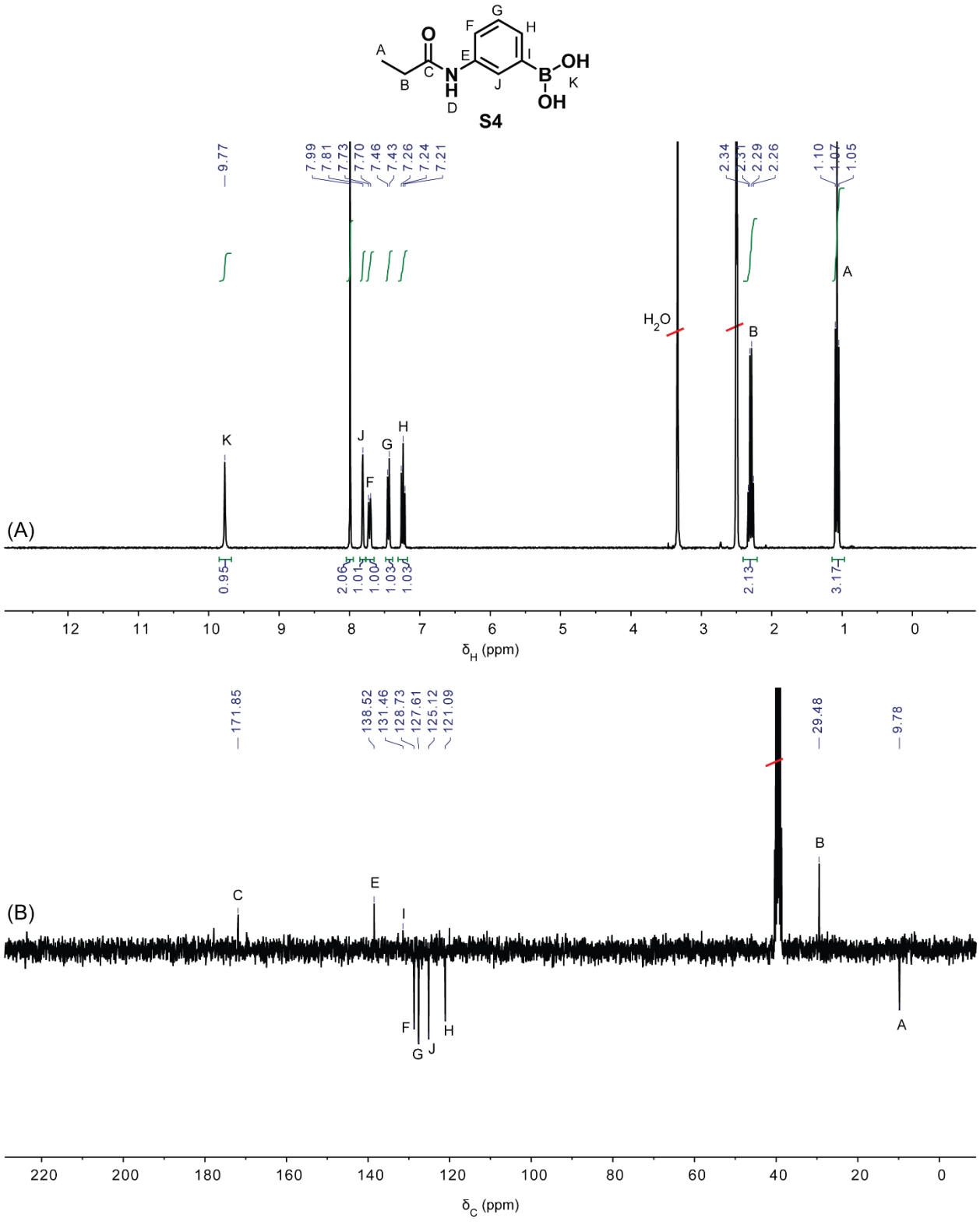

Figure S31 (**A**) ^{1}H NMR spectrum (DMSO-d_6, 500.1 MHz, 298 K) and (**B**) of ^{13}C NMR spectrum (DMSO-d_6, 75.5 MHz, 298 K) of **S4**.

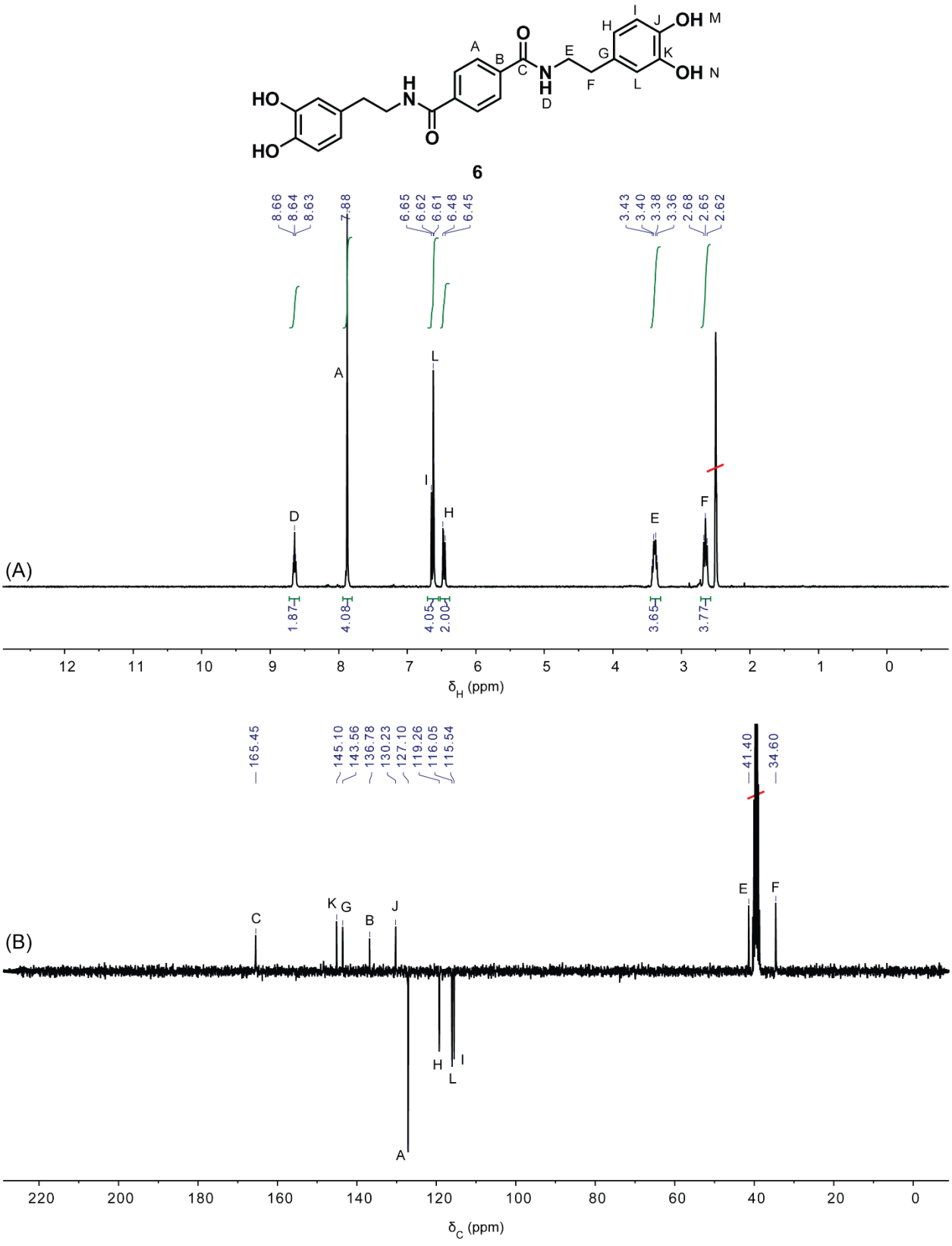

Figure S32 (**A**) ^{1}H NMR spectrum (DMSO-d_6, 300.1 MHz, 298 K) and (**B**) of ^{13}C NMR spectrum (DMSO-d_6, 75.5 MHz, 298 K) of **6**.

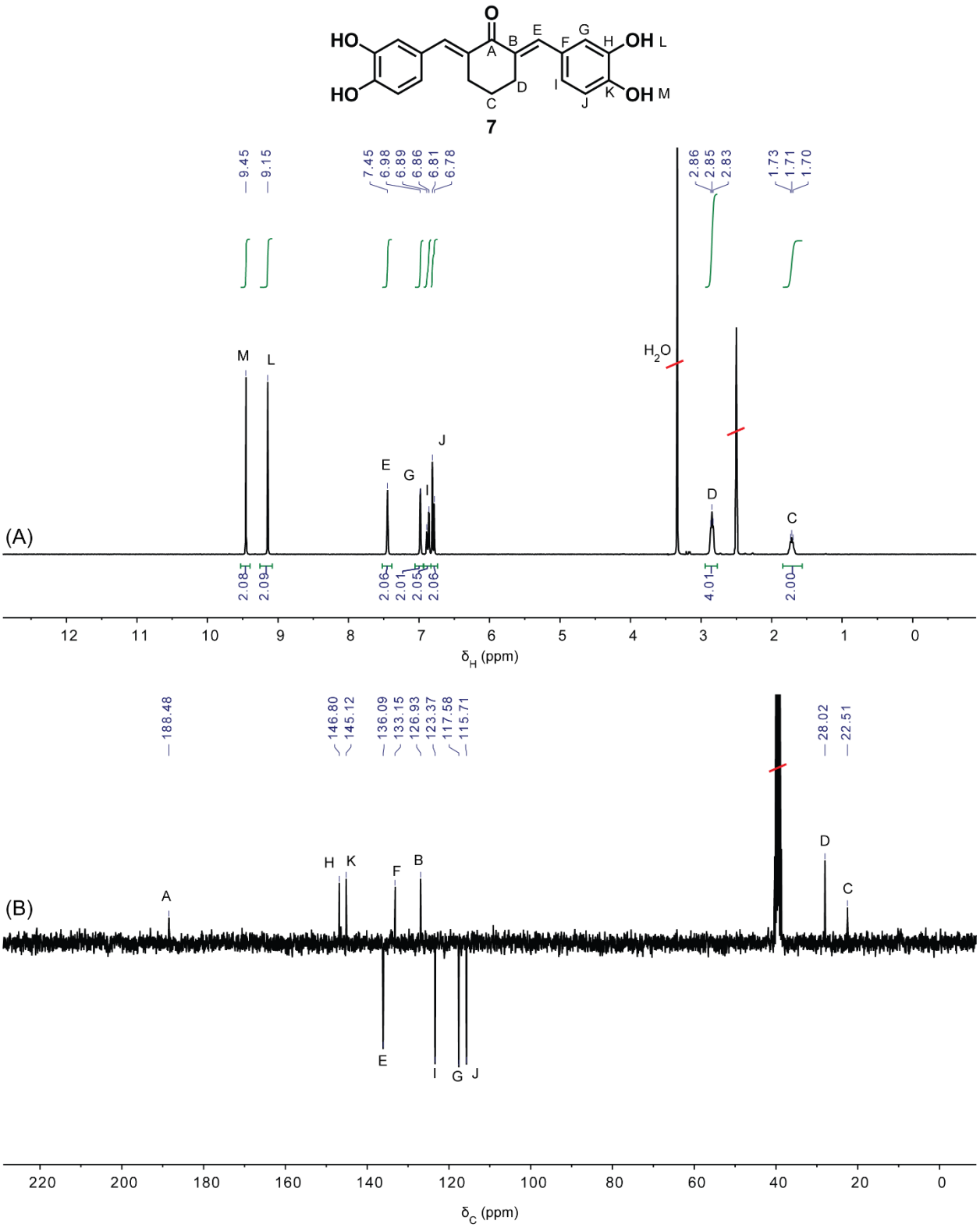

Figure S33 (**A**) ^{1}H NMR spectrum (DMSO-d_6, 300.1 MHz, 298 K) and (**B**) of ^{13}C NMR spectrum (DMSO-d_6, 75.5 MHz, 298 K) of **7**.

9. References

(S1) Locatelli, E.; Ori, G.; Fournelle, M.; Lemor, R.; Montorsi M.; Comes Franchini, M. *Chem. Eur. J.* **2011**, *17*, 9052–9056.

(S2) Hill, H. D.; Millstone, J. E.; Banholzer M. J.; Mirkin C. A. *ACS Nano*, **2009**, *3*, 418–424.

(S3) Sellers, H.; Ulman, A.; Shnidman Y.; Eilers, J. E. *J. Am. Chem. Soc.*, **1993**, *115*, 9389–9401.

(S4) Jain, P.K.; Huang, W.; El-Sayed, M. A. *Nano Lett.*, **2007**, *7*, 2080–2088.

(S5) Romo-Herrera, J. M.; Alvarez-Puebla, R. A.; Liz-Marzán, L. M. *Nanoscale*, **2011**,3, 1304–1315.